Journal Pre-proof

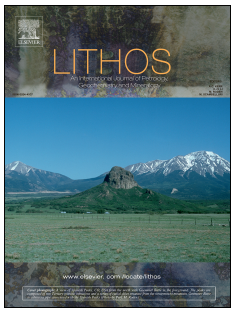

A review of molybdenite, and fluorite mineralization in Caledonian granite basement, western Ireland, incorporating new field and fluid inclusion studies, and Re-Os and U-Pb geochronology

Martin Feely, Alessandra Costanzo, Sean P. Gaynor, David Selby, Emma McNulty

PII: S0024-4937(19)30426-8

DOI: https://doi.org/10.1016/j.lithos.2019.105267

Reference: LITHOS 105267

To appear in: *LITHOS*

Received Date: 20 September 2019

Revised Date: 22 October 2019

Accepted Date: 28 October 2019

Please cite this article as: Feely, M., Costanzo, A., Gaynor, S.P., Selby, D., McNulty, E., A review of molybdenite, and fluorite mineralization in Caledonian granite basement, western Ireland, incorporating new field and fluid inclusion studies, and Re-Os and U-Pb geochronology, *LITHOS*, https://doi.org/10.1016/j.lithos.2019.105267.

A review of molybdenite, and fluorite mineralization in Caledonian granite basement, western Ireland, incorporating new field and fluid inclusion studies, and Re-Os and U-Pb geochronology.

Martin Feely[1]*, Alessandra Costanzo[1], Sean P. Gaynor[2,3], David Selby[4] and Emma McNulty[1]

[1] Geofluids Research Group, Earth and Ocean Sciences, School of Natural Sciences, National University of Ireland Galway, Galway, Ireland
[2]Department, of Geological Sciences, University of North Carolina at Chapel Hill, Chapel Hill, North Carolina, 27510, USA
[3]*Now at* Department of Earth Sciences, University of Geneva, rue des Maraîchers 13, Geneva, Switzerland
[4] Department of Earth Sciences, Durham University, Durham, UK

Abstract

The recent discovery of late-magmatic quartz vein hosted molybdenite, and exceptional gem quality vein fluorite, in the Caledonian Galway Granite Complex (GGC), has prompted a review of these contrasting styles of mineralisation in the late-Caledonian granite basement, Connemara, western Ireland. Existing published U-Pb and Re-Os chronometry and fluid inclusion microthermometry are combined with new: a) geological field observations, b) U-Pb zircon and Re-Os molybdenite geochronometry and c) fluid inclusion microthermometry to generate a new pressure-temperature-time model (P-T-t) of mineralization for the GGC. Re-Os chronometry molybdenite indicates that granite related molybdenite mineralisation extended from ~423Ma to ~380Ma overlapping with the GGC emplacement history determined by U-Pb zircon chronometry. The P-T-t model reflects initial granite emplacement and Mo-mineralisation at ~423Ma followed by lower P and T granite emplacement and related quartz vein hosted Mo-mineralisation at ~410Ma (Carna pluton), ~400Ma (Kilkieran pluton) and at ~380Ma (Costelloe Murvey granite). The gem quality fluorite veins in the GGC represent late-Triassic hydrothermal mineralisation that forms part of a regional N Atlantic-European Triassic-Jurassic hydrothermal mineralisation province triggered by the rifting of the N Atlantic facilitating crustal thinning and subsidence of

continental crust and initiating hydrothermal activity at the margins of Mesozoic basins thus facilitating hydrothermal vein fluorite mineralisation in, for example, the Caledonian GGC of western Ireland.

A review of molybdenite, and fluorite mineralization in Caledonian granite basement, western Ireland, incorporating new field and fluid inclusion studies, and Re-Os and U-Pb geochronology.

Martin Feely[1]*, Alessandra Costanzo[1], Sean P. Gaynor[2,3], David Selby[4,5] and Emma McNulty[1]

[1]Geofluids Research Group, Earth and Ocean Sciences, School of Natural Sciences, National University of Ireland Galway, Galway, Ireland
[2]Department, of Geological Sciences, University of North Carolina at Chapel Hill, Chapel Hill, North Carolina, 27510, USA
[3]*Now at* Department of Earth Sciences, University of Geneva, rue des Maraîchers 13, Geneva, Switzerland
[4]Department of Earth Sciences, Durham University, Durham, UK

[5] State Key Laboratory of Geological Processes and Mineral Resources, School of Earth Resources, China University of Geosciences, Wuhan, 430074, China

Abstract

The recent discovery of late-magmatic quartz vein hosted molybdenite, and exceptional gem quality vein fluorite, in the Caledonian Galway Granite Complex (GGC), has prompted a review of these contrasting styles of mineralisation in the late-Caledonian granite basement, Connemara, western Ireland. Existing published U-Pb and Re-Os chronometry and fluid inclusion microthermometry are combined with new: a) geological field observations, b) U-Pb zircon and Re-Os molybdenite geochronometry and c) fluid inclusion microthermometry to generate a new pressure-temperature-time model (P-T-t) of mineralization for the GGC. Re-Os chronometry molybdenite indicates that granite related molybdenite mineralisation extended from 423 to 380Ma overlapping with the GGC emplacement history determined by U-Pb zircon chronometry. The P-T-t model reflects initial granite emplacement and Mo-mineralisation at ~423Ma followed by lower P and T granite emplacement and related quartz vein hosted Mo-mineralisation at ~410Ma (Carna pluton), ~400Ma (Kilkieran pluton) and at ~380Ma (Costelloe Murvey granite). The gem quality fluorite veins in the GGC represent late-Triassic hydrothermal mineralisation. These veins form part

of a regional N Atlantic-European Triassic-Jurassic hydrothermal mineralisation province. Vein emplacement was triggered by the rifting of the N Atlantic facilitating crustal thinning and subsidence of continental crust and initiating hydrothermal activity at the margins of Mesozoic basins.

Keywords: Caledonian granite basement, late-magmatic molybdenite, Triassic hydrothermal fluorite

Introduction

One of the most significant and economically important types of mineralising fluid flow regimes in the crust are those related to granitic intrusions. Molybdenite mineralisation for example, is genetically related to granite magmatism. The Caledonian-Appalachian Orogen is marked by a ~50 m.y. period of granite intrusions with associated molybdenite mineralisation systems (**Ayuso, 1999; Plant, 1986; Whalen, 1993; Lynch et al. 2009**). Furthermore, granitic basement rocks invariably contain a variety of economic and sub-economic mineral and hydrocarbon deposits that postdate the crystalline host. Global occurrences of younger hydrothermal vein mineralising systems are well documented (*e.g.* **Chesley *et al.*, 1993; Munoz *et al.*, 1994; Halliday and Mitchell, 1984; Canals and Cardellach, 1993; McCaffrey *et al.*, 1999; Conliffe and Feely, 2010**), as are biogenic hydrocarbons in fractured granitic and other crystalline basement rocks (**Parnell, 1988; Petford and McCaffrey, 2003; Trice, 2014; Feely *et al.*, 2017; Holdsworth *et al.*, 2019**).

The recent discovery of quartz vein hosted molybdenite, and exceptional gem quality vein fluorite, in a working quarry (Larkin's Connemara Granite Quarry, Shannapheasteen), has prompted a re-investigation of these contrasting styles of

mineralisation in the late-Caledonian GGC of south Connemara. This quarry, like the one described by **O'Connor *et al.*, (1993**), also exposes a mid-Palaeozoic dike that is cut by millimetric scale veinlets of fluorite. Accordingly, existing published U-Pb and Re-Os chronometry and fluid inclusion microthermometry are combined with new geological field observations, U-Pb zircon and Re-Os molybdenite geochronometry and fluid inclusion microthermometry to generate a new P-T-t (Pressure-Temperature-time) regional scale model of late-magmatic Mo-mineralization and later hydrothermal fluorite mineralisation in the GGC.

The new data presented here provides supporting evidence for prolonged and episodic granite emplacement in tandem with granite related molybdenite mineralisation in the GGC and in other granites along the Caledonian-Appalachian orogen (Feely et al. 2010). The molybdenite in the GGC is an integral part of the granite related molybdenite mineralization corridor located along the Caledonian-Appalachian orogeny of the North Atlantic Massif. The fluorite mineralization in the GGC is broadly synchronous with other Triassic-Jurassic hydrothermal vein mineralisation throughout the North Atlantic margins and Europe and forms part of a hydrothermal province identified by Mitchell and Halliday (1976).

Regional Setting of the Galway Granite Complex

The GGC occupies a key location in the Appalachian-Caledonian orogenic belt. The 80 km long, WNW-trending axis of the GGC lies astride and stitches the EW-trending Skird Rocks Fault, a splay of the orogen-parallel Southern Uplands Fault (**Leake, 2006**). The Skird Rocks Fault brings amphibolite facies rocks of the Grampian Connemara Metamorphic Complex against the Lower Ordovician greenschist-facies rocks of the South Connemara Group. The Connemara Metamorphic Complex

comprises Lower to Upper Dalradian greenschist to amphibolite facies rocks, intruded by a) the Grampian phase 470–465Ma Metagabbro-Gneiss Suite, then by b) the Oughterard Granite (~463Ma) and c) the Silurian-Devonian GGC (~425–380Ma) (**Leake, 1989; Leake and Tanner, 1994; Friedrich *et al.*, 1999a, b; Pracht *et al.*, 2004; Feely *et al.*, 2006; Leake, 2006; Feely *et al.*, 2010; Dewey and Ryan, 2016; Friedrich and Hodges, 2016; Feely *et al.*, 2018).** In the north, the Dalradian metasediments are overlain by Silurian strata (**Leake and Tanner, 1994**) and in the south Lower Ordovician greenschist facies rocks (the South Connemara Group) are intruded by the GGC (**McKie and Burke, 1955; Williams *et al.*, 1988**). The Delaney Dome Formation, is a 474.6 ± 5.5 Ma metavolcanic complex (**Leake and Singh, 1986; Draut and Clift, 2002)**. To the east the metamorphic and igneous rocks of the Connemara region are in faulted contact with Carboniferous Limestones (**Lees and Feely, 2016 and 2017**) - see **Figure 1.**

Molybdenite, and fluorite mineralisation in the GGC-a research history

The well-exposed Silurian-Devonian GGC provides a unique opportunity to study the temporal and spatial relationships of late-magmatic Mo-mineralisation (with associated chalcopyrite), and the later hydrothermal fluorite veins that can include varying proportions of galena, sphalerite, chalcopyrite/pyrite, calcite, barite and quartz. Indeed, numerous studies of the spatial distribution and structural controls of the Mo-mineralisation in the GGC were published in the late 20th Century *e.g.*, **Derham (1986); Max and Talbot (1986); Derham and Feely (1988); McCaffrey *et al.* (1993)**. In addition, fluid inclusion microthermometry combined with stable isotope studies (O, H, S, C) were used to investigate the genesis of the Mo-mineralisation (**Feely and Hoegelsberger, 1991; Gallagher *et al.*, 1992; O'Reilly *et***

***al.,* 1997**). The results of a regional fluid inclusion study by **O'Reilly *et al.* (1997)** and later supported by **Feely *et al.*, (2007)**, show that late-magmatic, high-T (~450^{o}C) low to moderate salinity (4–10 eq. wt% NaCl) aqueous-carbonic fluids were associated with the Mo-mineralisation. A second, aqueous fluid, of lower–T (~270–340^{o}C) and low to moderate salinity (0–10 eq. wt.% NaCl) is ubiquitous throughout granite and vein quartz in the GGC and is interpreted to reflect mixing between late magmatic and meteoric fluids. Finally, microthermometry shows that fluid inclusions associated with the fluorite mineralization veins are $CaCl_2$ bearing and more saline (8–28 eq. wt.% NaCl) and have lower temperatures (~125–205^{o}C) than the earlier fluids. Furthermore, **Jenkin *et al.* (1997)** noted that pressures during the deposition of these late-Triassic fluorite veins were <0.7 kb. **Conliffe and Feely (2010)** in their regional study of fluid inclusions hosted by granite quartz in onshore Irish granite basement recorded the presence of these fluids, arguing that they represent mixing between meteoric and basinal fluids probably of Carbonifeous to Triassic in age. It is also noteworthy that **Conliffe *et al.*, (2010)** described similar fluids in sandstones from offshore Irish Mesozoic basins.

Many of the early fluid inclusion studies were based upon the assumption that the whole of the GGC was ~400Ma in age and that therefore the Mo-mineralization was also ~400Ma in age. **Leake and Tanner (1994)** for example, observed that the whole suite of plutons making up the GGC were late Caledonian and approximately 400Ma old. New geochronology studies, using the U-Pb zircon and Re-Os molybdenite chronometers have shown that the assembly of the GGC involved five main magmatic episodes extending from 423 to 380Ma (**Buchwaldt *et al.*, 2001; Feely *et al*,. 2003; Selby *et al.*, 2004; Feely *et al.*, 2007; Feely *et al.*, 2010; Feely *et al.*, 2018)**. The earliest magmatic episode ~423Ma was marked by the emplacement of the Omey,

Inish and Roundstone Plutons. These were followed by the Carna Pluton (~410Ma), the Kilkieran Pluton (~400Ma), then later intrusions at ~380Ma *e.g.*, Costelloe Murvey granite (**Feely *et al.*, 2010) – see Figure 1**. Finally, mid-Palaeozoic composite dolerite-rhyolite diking represents the last magmatic episode **(Mohr, 2004; Mohr *et al.*, 2018**). **Feely *et al.*, (2010**) have shown that the temporal assembly of the GGC reflects episodic and long-lived granite emplacement (~40Ma) in tandem with granite-related Mo-mineralization.

The GGC hosts numerous fluorite veins that contain a combination of the following minerals: chalcopyrite, galena, pyrite, quartz, calcite, barite and chlorite – see **O'Raghallaigh *et al.* (1997)** for a spatial distribution map together with descriptions of the fluorite veins. More recently Moreton and Lawson (2019) described fluorite and associated minerals from the Lettermuckoo quarry in the GGC. **O'Connor *et al.*, (1993**) reported that vein fluorite not only postdates the GGC, but also cuts a dolerite dike in the Costelloe Murvey granite quarry **(Figure 1)**. The results of fluid inclusion studies of the vein fluorite, fluorite rare earth element (REE) abundances modelling and ^{40}Ar-^{39}Ar geochronometry of the dolerite dike by **O'Connor *et al.*, (1993)** concluded that the dolerite dike emplacement and the transecting fluorite mineralisation occurred in mid-Triassic times triggered by continental rifting of the Atlantic margin in western Ireland. However, subsequent studies by **Jenkin *et al.*, 1997; Menuge *et al.*, 1997; O'Reilly *et al.*, 1997; and Jenkin *et al.*, 1998** proposed that the mid-Triassic age determined by **O'Connor *et al.*, (1993)** for the dike reflects the timing of the hydrothermal fluorite mineralisation only. Recently, **Mohr *et al.*, (2018)** re-investigated the age of the dolerite dike populations in south Connemara and noted that the pervasive hydrothermal alteration of the mid-Palaeozoic (late Devonian) dolerite dikes in the GGC, including that from **O'Connor *et al.*, (1993)**, is

linked to the hydrothermal fluorite mineralization.

The geological setting of the samples from Larkin's Connemara Granite Quarry.

Larkin's Connemara Granite Quarry (53°20'19''N; 9°26'29''W) in Shannapheasteen, south Connemara, covers an area of ~ 200m x 170m and is ~50m east of the R372 (**Figure 2**). It is located within the area mapped by **Leake (2006)** as the Shannapheasteen Finegrained (0.5-1.5mm) Granite (SFG) which is very poorly exposed. This SFG intrudes the Kilkieran pluton by block stoping **(Leake, 2006).** Larkin's quarry is located on an stoped block of the Kilkieran Pluton's foliated Porphyritic Granite whose main exposure occurs c.250 m to the west. The quarry has been in operation for ~10 years and the foliated quarry granite is used for road construction and hard landscaping in the region. The quarry granite type is light grey, coarse grained (0.5–1.5cm) and inequigranular and porphyritic with approximately 30 vol.% quartz, 40 vol.% plagioclase, 20 vol.% K-feldspar and 10 vol.% biotite. It has a well developed vertical-dipping biotite fabric (**Figure 3a**). The granite, technically a granodiorite (**Streckeisen, 1967**), is cut by: ***1)*** a ~10 cm wide molybdenite bearing quartz vein (**Figure 3b**). The vein is exposed along strike for c.2m and the molybdenite mainly occurs along the vein wall, ***2)*** a c. 50cm wide quartz porphyry dike (**Figure 3c**) can be mapped discontinuously along strike for ~100m. It is cut by the fluorite vein and and the dolerite dike. The latter offsets the porphyry, in a sinistral sense by ~20m. Centimetric scale fluorite veins transect the porphry close to the main fluorite vein. ***3)*** the NW trending, ~1.5m wide, vertical dolerite dike (**Figure 3d**) extends the length of the quarry and is deeply weathered. Millimetric scale fluorite veinlets also cut the dolerite. ***4)*** A NW trending ~5m wide fluorite vein (**Figure 3e**) that extends beyond the quarry's boundary. The descriptive 'fluorite vein' does not

adequately describe this mineralised structure. It is a fluorite-bearing granodiorite breccia. The breccia is composed of angular and sub-rounded blocks of the host granodiorite that range up to 0.5 metre in their longest dimension. The granite blocks have not been significantly rotated. It is similar to a crackle breccia which is defined as a type of breccia where the clasts have been separated by planes of rupture but have experience little or no displacement (Shukla and Sharma, 2018). Vugs, containing exceptional gem quality fluorite crystals, occur between the granite blocks. This type of structure is similar to the Green Ridge Breccia in the Snoqualmie Granite of the Cascades (**Feely *et al.*, 2017**) where gem quality amethyst bearing vugs cement brecciated host granite blocks. The gem fluorite occurs as cubes, octahedra, dodecahedra and in combinations of these crystal forms. The colours of the fluorite range from clear to deep purple and green hues. Crystallographically controlled colour zoning displaying deep purple and relatively clear zones are common especially in the combination forms (**Costanzo and Feely, 2019**; **Figure 4)**.

In summary, field relationships indicate that the quartz porphyry dike and the Mo-bearing quartz vein are related to the granodiorite. The fluorite mineralisation is the youngest event because the dolerite dike, and indeed the granodiorite related quartz porphyry dike, are cut by millimetric to centimetric scale veins of fluorite.

Three samples were taken for geochronology and fluid inclusion studies (see below). An additional Mo bearing quartz vein sample, GBM, from the Costelloe area (**Figure 1**) is included in this study. Sample GBM is from a NE striking vertical 2 cm thick quartz vein that along its wall contains abundant molybdenite and chalcopyrite both of <3mm grain size. The quartz vein can be traced along strike for □5 m and cross-cuts a coarse grained (5–10 mm) granodiorite in the Kilkieran pluton. A molybdenite Re-Os age of ~383Ma (youngest age yet determined for molybdenite in the GGC) has

already been published by **Feely *et al.* (2010)** from this vein and we use this opportunity to present new fluid inclusion microthermometry from the vein quartz.

Sampling and Analytical Methods

Three samples were taken for geochronology and fluid inclusion studies *i.e.* LQ-1: the quarry granodiorite (U-Pb zircon chronometry); LQ-2: the Mo-bearing quartz vein (Re-Os chronometry and vein quartz fluid inclusion microthermometry), LQ-3: vein fluorite for fluid inclusion microthermometry and GBM from the Costelloe area (fluid inclusion microthermometry of vein quartz).

Zircon U-Pb Geochronology

A 5kg sample of the quarry granodiorite (LQ-1) was analyzed for U-Pb Chemical Abrasion Isotope Dilution Thermal Ionization Mass Spectrometry (CA-ID-TIMS) zircon geochronology. The sample was prepared at the University of North Carolina (UNC), Chapel Hill, USA, by crushing using a jaw crusher and a disc mill. Zircons were isolated using standard density (water table and heavy liquids) and magnetic separation techniques. Individual zircon grains were selected using a binocular microscope to represent the size and morphology range present in the samples. Selected zircon grains were thermally annealed for 48 hours at 900°C and then chemically abraded for 4 hours at 220°C in order to eliminate volumes affected by radiation damage and to remove inclusions (**Mundil *et al*., 2004; Mattinson, 2005**). Abrading the zircons for additional time caused complete dissolution of the grains, due to their metamict characteristics. All zircon analyses were of single crystals. Zircons were spiked using a ^{205}Pb-^{233}U-^{236}U tracer (**Parrish and Krogh, 1987**) and dissolved following a procedure modified after **Krogh (1973**) and **Parrish (1987**). U and Pb were isolated using HCl anion exchange chromatography procedures modified

after **Krogh (1973**). Isotope ratios of both U and Pb were determined by thermal ionization mass spectrometry (TIMS) on an Isotopx Phoenix mass spectrometer at UNC, Chapel Hill. Uranium was run as an oxide after loading in silica gel on single Re filaments. Lead was loaded in silica gel on single zone-refined Re filaments. Both U and Pb were analyzed in single-collector peak-switching mode using a Daly ion-counting system. In-run U fractionations were calculated based on the measured value for $^{233}U/^{236}U$ in the spike, and Pb fractionation was estimated to be 0.15%/amu based on replicate analyses of NBS 981. Data processing and age calculations were completed using the applications Tripoli and U-Pb Redux (**Bowring *et al.*, 2011; McLean *et al.*, 2011**). Decay constants used were $^{238}\lambda=1.55125E^{-10}$ and $^{235}\lambda=9.8485E^{-10}$ (**Jaffey *et al.*, 1971**).

Molybdenite Re-Os Geochronology

A 2 kg sample of vein quartz (LQ-2), that hosts fine-grained (2-4 mm) disseminations of molybdenite, was sent to Durham University for molybdenite Re–Os geochronometry in the Laboratory for Source Rock and Sulfide Geochemistry and Geochronology and the Arthur Holmes Laboratory. Detailed sample preparation and analytical protocols are given by **Selby and Creaser (2001); Selby and Creaser (2004); Selby *et al.*, (2007); Lawley and Selby (2012)**. In brief, molybdenite was isolated from the quartz vein using traditional mineral separation techniques (crushing, Frantz magnetic separation, heavy liquids [MI and LST], and water floatation). Additional purification (removal of remaining silicates) was achieved using a room temperature HF dissolution (**Lawley and Selby, 2012**). An aliquant (~30mg) of the molybdenite separate was digested in a 3:1 mix of HNO_3:HCl (inverse *aqua regia*) with an known amount of mixed isotope tracer (^{185}Re and normal Os) in a carius tube at 220ºC for 24 hrs. Osmium was purified from the acid mix using solvent

extraction ($CHCl_3$) and micro-distillation methods. Rhenium was purified using NaOH-acetone solvent extraction and anion chromatography (Li *et al*., 2017). The purified Os and Re were loaded to Pt and Ni filaments, respectively. The isotope ratios were measured using Negative Thermal Ionization Mass Spectrometry on a Thermo Scientific TRITON mass spectrometer using Faraday collectors. Although insignificant compared to the Re and ^{187}Os abundance in the molybdenite sample, all data was blank corrected (Re = 2 picograms (pg); Os = 0.1 pg, with an $^{187}Os/^{188}Os$ blank composition of 0.17 ± 0.02, n = 1). The Re-Os uncertainties are reported at the 2σ absolute level, which were determined through error propagation of uncertainties related to Re and Os mass spectrometer measurements, tracer calibration, sample and tracer solution weight, reproducibility of Re and Os standards, as well as uncertainties related to the blank determination. Results of analyses of the Henderson molybdenite reference material (RM8599 - 27.695 ± 0.038 Ma) reported by **Li *et al.* (2017**) overlap with the analysis of this study. A ^{187}Re decay constant of $1.666\times10^{-11}\ y^{-1}$ with an uncertainty of 0.31% was used in the calculation of the Re-Os dates (**Smoliar *et al*., 1996; Selby *et al*., 2007**).

Fluid inclusion studies

Transmitted polarised light microscopy was used to establish a fluid inclusion classification scheme. Microthermometric analyses of suitable fluid inclusions hosted by the molybdenite bearing vein quartz (LQ-2 and GBM) and vein fluorite (LQ-3) were then carried out at the Geofluids Research Laboratory, National University of Ireland, Galway, Ireland. Doubly polished fluid inclusion wafers of each of the samples (~100μm thick) were studied using a Linkam THMGS 600 heating-freezing stage, mounted on an Olympus transmitted light microscope. The instrument was calibrated according to the method outlined by **MacDonald and Spooner (1981**)

using synthetic fluid inclusion standards (pure CO_2 and water). Precision is ± 0.2°C at -56.5°C and ± 0.5°C at 300°C. The microscope is equipped with a range of special extra-long working distance objective lenses ranging up to x100 magnification.

Results

Zircon U-Pb Geochronology

Individual zircons separated for this study were fairly metamict, commonly hosted inclusions and ranged from 90 to 210 µm along the elongate axis prior to chemical abrasion. All zircon U-Pb ages reported in this study are concordant within analytical and decay constant uncertainties (**Figure 5; Table 1**). T_H-corrected $^{206}Pb/^{238}U$ zircon age determinations are used for all interpretations because this chronometer provides the most precise and accurate estimate for rocks of this age (e.g., Schoene, 2014). Individual zircon grains from the quarry granodiorite (LQ-1) yield $^{206}Pb/^{238}U$ ages ranging from 407.28 to 401.06 Ma, with six grains overlapping within uncertainty at 401.89 Ma and three older grains (407.28, 406.56 and 405.76 Ma).

Molybdenite Re-Os Geochronology

The molybdenite sample LQ-5-2 possesses ca. 161 ppm Re and 680 ppb ^{187}Os (**Table 2**). The ^{187}Re and ^{187}Os molybdenite data yield a Re-Os model date of 401.0 ± 0.2/1.6/2.0 Ma (uncertainties presented as analytical /+ tracer /+ decay constant uncertainties; **Table 2**).

Fluid inclusion microthermometry

Four principal types of fluid inclusions (*i.e.* Type 1, 2, 3 and 4) have been observed based upon the number of phases (liquid [L]; vapour [V]; solid [S]) present at room temperature (~20^{o}C) (**Table 3)**.

Type 1 inclusions are two phase (L+V; L>V) aqueous inclusions and they are recorded in all samples. The degree of fill, F (F = vol. of liquid/ [vol. of liquid + vapour]) of Type 1 inclusions is ~0.7–0.9. The inclusions occur either as isolated individuals, in clusters or in trails. Their size ranges from 2 to 20µm in their longest dimension (fluorite hosted FIs range up to ~200 microns) and display a range of morphologies, varying from negative crystal shape to rounded morphologies. Type 1 are the dominant petrographic type in the molybdenite vein quartz samples LQ-2 and GBM and in the vein fluorite sample LQ-3.

Type 2 are monophase (L) aqueous inclusions and display rounded to negative crystal shape morphologies and range from 2 to 20µm (vein fluorite Type 2 range up to 100 microns) in their longest dimension. They occur as clusters of individuals or as trails in all samples.

Type 3 are multi-phase (L + V + S) aqueous inclusions. They are generally rounded in shape and range from 5 to 20µm (but can range up to 200µm) in their longest dimension. They are only observed in the fluorite where they occur in trails and clusters.

Type 4 are two phase (L+ S) aqueous inclusions. They display rounded to negative crystal shape morphologies and range from 5 to 100µm in longest dimension. They occur in clusters or trails and are only observed in the vein fluorite.

Type 1 two-phase aqueous primary (using the petrographic criteria of **Roedder, 1984**) fluid inclusions were chosen for microthermometry **(Figure 6)** and isochore based

pressure-temperature modeling. On freezing of the Type 1 inclusions to -110°C and subsequent heating the temperature of eutectic melting, the temperature of hydrohalite melting (T_{Mhyd}), the temperature of last ice melting (T_{LM}) and the temperature of liquid to vapour homogenization (temperature of homogenization T_H) were measured. Type 1 inclusions hosted by the vein fluorite commonly showed eutectic melting of ~ -52ºC indicating the presence of $CaCl_2$ in addition to NaCl. The "crazy paving" texture that reflects first melting at the H_2O-NaCl-$CaCl_2$ ternary minimum **(Shepherd *et al.*, 1985)** was observed in many of the fluorite hosted primary Type 1 inclusions. Last hydrohalite ($NaCl.2H_2O$) melting temperatures and last ice melting temperatures (T_{LM}) were obtained by the method of sequential heating (**Shepherd *et al.*, 1985**). The microthermometric data was then used to calculate fluid compositions in the system $CaCl_2$-NaCl-H_2O (**Steele-MacInnis, *et al.*, 2011**). Furthermore, Type 1 fluid inclusions that displayed eutectic melting at ~-25°C to ~ -20°C indicate general fluid compositions varying from NaCl+KCl+H_2O to NaCl+H_2O. T_{LM} values were used to calculate salinities (eq. wt.% NaCl), using the equations of **Bodnar (1993)**. On heating of the inclusions, the temperature of homogenization (T_H), always to the liquid phase, was recorded. In general, the T_H represents the minimum temperature of fluid trapping. **Table 4** presents a summary of the microthermometric data obtained for the Type 1 primary fluid inclusions in the three samples. Bivariate plots of T_H and salinity (eq. wt.% NaCl) for the Type 1 fluid inclusions trapped in the two molybdenite vein quartz samples (LQ-2 and GBM) and vein fluorite (LQ-3) are presented in **Figure 7**. **Figure 7** also displays, for comparative purposes, the fields defined by the three main fluid types recorded in the GGC by **Feely and Hogelsberger (1991), Gallagher *et al.* (1992) O'Reilly *et al.* (1997) and Jenkin *et al.* (1997).** The Type 1 FIs trapped in the molybdenite vein quartz samples display a similar range of T_H values (~180-280°C),

however, GBM FIs display a broader range of salinities i.e. ~4.0–10.0 eq. wt. % NaCl compared to LQ-2 (~0.4–5.0 eq. wt.% NaCl). The microthermometric data for the Type 1 FIs in both Mo-bearing quartz veins plot outside and below the field defined by the late magmatic aqueous-carbonic fluids associated elsewhere in the GGC with the Mo-mineralization. Indeed they plot in the field defined by **O'Reilly *et al.* (1997)** as representing magmatic heat-driven convection of meteoric fluids mixing with late magmatic fluids into the granite.

Type 1 fluid inclusions hosted by the vein fluorite have significantly higher salinities (~10–25 eq. wt.% NaCl) and lower T_H values (~100–200°C). These are broadly similar to those values recorded from the vein fluorite that cuts the Costelloe Murvey granite (CMG) and the dolerite dike in the CMG quarry (**O'Connor *et al.*, 1993**). The variation in salinity and T_H displayed by these fluorite hosted Type 1 fluid inclusions overlap with the field that according to **O'Reilly *et al.* (1997)** and **Jenkin *et al*. (1997)** reflect the mixing of a high T meteoric fluids with a lower T and high salinity basinal brine (**Figure 7**). **O'Reilly *et al.* (1997)** and **Jenkin *et al*. (1997)** argued, using fluid inclusion and stable isotope data that the hydrothermal fluids responsible for deposition of the fluorite veins in the GGC (like the LQ-3) involved the mixing of two main fluid types. These were a meteoric, high-T (~205°C) and moderate salinity (~12 eq. wt% NaCl) fluid probably of late-Triassic age mixing with a lower T (~125°C) high salinity (>21 eq. wt% NaCl) fluid interpreted as a basinal brine from Lower Carboniferous sediments. The calculated $CaCl_2$-NaCl-H_2O compositions of Type 1 inclusions hosted by the vein fluorite from Larkin's quarry, and for comparison, from the CMG quarry, are shown in **Figure 8**. In general, there is an overlap in fluid composition ranges from the two fluorite vein localities. Furthermore, the fluid compositions from these two locations plot in the composition field of granite quartz

hosted fluids interpreted by **Conliffe and Feely, (2010**) as reflecting incursions of Carboniferous and/or Triassic fluids into onshore Irish granite basement.

Discussion

Interpretation of Zircon Geochronology Data

The zircon U-Pb data presented in this study span a range beyond the uncertainty of individual analyses. This is a common feature of modern CA-ID-TIMS U-Pb zircon datasets, as technical developments have permitted the reduction of uncertainties on individual analyses (*e.g.* **Samperton *et al.*, 2015; Widmann *et al.*, 2019**). There are several models to interpret an age from such chronology data: (1) zircon antecrysts are abundant in igneous rocks, and therefore, only the youngest grain reflects crystallization at the emplacement level (*e.g.*, **Schaltegger *et al.*, 2009**); (2) protracted magma crystallization is recorded by the entirety of the zircon spectrum, therefore the entire age range reflects the age of the rock (*e.g.*, v**on Quadt *et al.*, 2011; Wotzlaw *et al.*, 2013**); and (3) samples can contain both antecrystic grains and grains suffering from Pb-loss (*e.g.*, **Ovtcharova *et al.*, 2015**). The zircon age spectra for the sample of this study is best categorized as two distinct populations, at approximately ~406.5 and 402 Ma, with no overlap. Therefore it is most likely that either the older population reflects antecrystic grains or the younger population has undergone Pb-loss and is artificially young. As it is highly unlikely that Pb-loss would affect multiple grains with precisely the same isotopic offset towards a young age, we interpret that the older apparent ages to reflect the presence of antecrysts. Antecrystic zircon are not uncommon amongst porphyritic intrusions, and have been identified in multiple other CA-ID-TIMS studies of intrusions associated with mineralization (*e.g.*, **Chelle-Michou *et al.*, 2014; Buret *et al.*, 2017; Gaynor *et al.*, 2019**).

The remaining six, younger grains overlap and are normally distributed around a mean value, however calculating a weighted mean age with all six grains yields a MSWD of 4.0. While all of the grains overlap within uncertainty of the mean of 401.89 ± 0.33Ma, the high MSWD value suggests these grains may not represent a single population. As such, we suggest there are two possible ways to interpret this age distribution: (1) that subtle amounts of antecrystic inclusions within the age spectra bias the age towards an older age (2) that the two youngest reflect subtle amounts of Pb-loss, artificially generating a younger age. The first interpretation yields a weighted mean age of 401.08 ± 0.54 Ma (MSWD =0.01), and the second yields a weighted mean age of 402.39 ± 0.42 Ma (MSWD = 1.8). Both of these situations to cause similar age spectra from other igneous zircons associated with alteration (*e.g.*, **Chelle-Michou *et al.*, 2014; Ovtcharova *et al.*, 2015; Buret *et al.*, 2017; Gaynor *et al.*, 2019**). There are no aspects of this dataset which could indicate one specific interpretation to be more geologically accurate, and both interpretations overlap with the weighted mean age calculated using all grains. Therefore we instead accept the weighted mean and uncertainty of all ~402 Ma as the preferred age for the quarry granodiorite sample LQ-1, 401.89 ± 0.33Ma, as a more inclusive interpretation of a complicated zircon age spectra.

Re-Os molybdenite age.

Including uncertainties, the new Re–Os molybdenite age (401.0 ± 0.2/1.6/2.0 Ma) for the LQ-5-2 Mo bearing quartz vein from Larkin's quarry is in excellent agreement with the U-Pb zircon age (401.89 ± 0.33 Ma) for the host granodiorite LQ-1.

Fluid inclusion microthermometry

The high-T, moderate salinity aqueous carbonic fluids associated with Mo-mineralization (Feely and Hogelsberger, 1991, **Gallagher *et al.*, 1992, O'Reilly *et al.*, 1997** and **Feely *et al.*, 2007)** were not encountered in the Mo-bearing LQ-2 and GBM quartz veins. The Type 1 moderate-T and low-moderate salinity (1–10 eq. wt.% NaCl) FIs recorded in the two veins (LQ-2 and GBM) are directly comparable to the two-phase aqueous inclusions of low to moderate salinity recorded throughout the GGC (Feely and Hogelsberger, 1991; **Gallagher *et al.*, 1992; O'Reilly *et al.*, 1997** and **Feely *et al.*, 2007).** The apparent absence of aqueous-carbonic fluids in the LQ-2 and GBM samples is in keeping with **O'Reilly *et al.* (1997)** who noted the rare occurrence of carbonic-rich fluid inclusions east of the Shannawona Fault (SF) in the GGC. The exposed deeper levels of the GGC east of the SF **(Leake, 2006**) may account for the scarcity of CO_2-bearing fluids, since they will tend to concentrate at higher levels within a batholith. However, the evidence here suggests that the presence of aqueous – carbonic fluids is not essential for molybdenite mineralisation. The lower T, $CaCl_2$-bearing aqueous fluids of moderate-high salinity (10-25 eq. wt.% NaCl) encountered in the vein fluorite samples (LQ-3 and COS-2 and COS-4) are similar to the late Triassic fluids described by **O'Reilly *et al.* (1997) and Jenkin *et al.*, (1997)**.

The Molybdenite mineralization

The molybdenite Re–Os and zircon U-Pb chronometry shows that the Mo-mineralization (LQ-2) is essentially contemporaneous with the crystallization of the host quarry granodiorite (LQ-1) at □401 Ma. Therefore, the timing of Type 1 fluid entrapment in LQ-2 is also □401 Ma. Furthermore, the Type 1 fluids in the GMB quartz vein were trapped at ~380 Ma, the age of the molybdenite mineralization **(Feely *et al.*, 2010)**. The computer program FLUIDS **(Bakker, 2003)** was used to

generate isochores in P-T space for the Type 1 aqueous fluids in both samples **(Figure 9)**. **Feely *et al.*, (2007)** determined a molybdenite Re-Os age of ~423 Ma for molybdenite bearing quartz veins in the Omey pluton and presented a P-T model for Mo mineralization using fluid inclusion microthermometry and aureole pressure constraints of 2.50 ± 0.25 kbar from **Ferguson & Al-Ameen (1985)** - see **Figure 9**. Previously, **Gallagher *et al.* (1992)** used fluid inclusion microthermometry and stable isotope data to generate a P-T model for Mo mineralization (Re-Os molydenite age □410 Ma, **Selby *et al.*, 2004**) in the Carna pluton, which yielded pressures of 1.2-2.0 kbar and a temperature range of 360–450°C (**Figure 9**). A higher pressure and lower temperature regime prevailed during Mo-mineralization, in the Omey pluton which was followed by a lower pressure and higher temperature regime during Mo-mineralisation in the younger Carna pluton (see **Figure 9**). The isochores for LQ-2 (Re-Os age ~401 Ma) and GMB (Re-Os age ~383 Ma) plot to the left of the Carna pluton's P-T field suggesting isobaric (assuming a P regime similar to the Carna pluton field) shifts to lower T conditions with increasingly younger phases of plutonism and accompanying Mo-mineralization.

The hydrothermal fluorite mineralization

Isochores for fluorite veins that postdate dolerite diking in the GGC are presented in **Figure 9**. The samples are a) vein fluorite sample LQ-3, b) vein fluorite sample COS-2, that cuts the dolerite dike in the CMG quarry and c) vein fluorite sample COS-4, that cuts the CMG in the same quarry. The latter two isochores are redrawn using microthermometric data for COS-2 and COS-4 in **O'Connor *et al.* (1993).** The dolerite dikes are members of the mid-Palaeozoic (Late Devonian?) dike suite **(Mohr *et al.*, 2018)** that transect the GGC. **O'Connor *et al.* (1993)** reported a Triassic $^{40}Ar/^{39}Ar$ age (~233Ma) for this dolerite dyke which is cut by the fluorite vein COS-2.

However, this age for dike emplacement was reinterpreted as reflecting late-Triassic hydrothermal mineralisation which was responsible for fluorite veining and perturbation of the dolerite chronometers *e.g.* $^{40}Ar/^{39}Ar$ (**Jenkin *et al.*, 1997, 1998, Menuge *et al.*, 1997 and Mohr *et al.*, 2018)**. The isochores plot to the left of the GGC P-T field in **Figure 9** and are constrained by an assumed lithostatic pressure of ~1kbar equivalent to a sedimentary cover over the GGC, of ~3.5km proposed by **O'Connor *et al*. (1993)** and is in keeping with the late-Triassic pressure constraint of ~0.7kbar proposed by **Jenkin *et al.* (1997).**

Summary and conclusions

The field relationships exposed in Larkin's quarry encapsulates a geological history of granite emplacement (Kilkieran pluton) at ~400 Ma, penecontemporaneous molybdenite mineralisation and porphyry dike emplacement. The dolerite dike was likely emplaced during late Devonian times (305 Ma?). During the late Triassic, vein fluorite±galena±chalcopyrite±sphalerite±calcite±quartz±barite) mineralization occurred forming in this instance a crackle breccia, maybe due to lithostatic pressure being less than hydrothermal fluid pressure during tectonic activity (**Shukla and Sharma, 2018**). The angular centimetric scale granite blocks are cemented together by vuggy gem quality hydrothermal fluorite. Fluorite veining also occurs in the deeply weathered dolerite dike and the granite related porphyry dike. Fluid inclusion studies show that the Mo mineralisation (LQ-2 and GBM) was depositied during mixing of late magmatic and meteoric fluids of moderate T (~250°C) and moderate–low salinity (<10 eq.wt.% NaCl). Fluorite (LQ-3) hosted fluid inclusions yield microthermometric data in keeping with evidence of fluid mixing between basinal brines and meteoric waters.

A P-T-t model **(Figure 9)** tracing the spatial and temporal development of late magmatic and hydrothermal mineralisation in the GGC shows that Mo mineralisation occurred in tandem with the plutonic assembly of the GGC. Combined fluid inclusion data, and U-Pb and Re-Os geochronometry have shown that prolonged granite-related molybdenite mineralization in the GGC was initiated in the NW by the emplacement of the Omey Granite at ~423 Ma, and then to the SE by the Carna (at ~410 Ma) and Kilkieran (at ~400 Ma) plutons and finally by the 380 Ma Costelloe Murvey granite (**Feely *et al.*, 2007; 2010**). Furthermore, the P-T model in **Figure 9** plots a change with time in P-T conditions from the NW to the SE as the GGC assembled over a period of ~40 million years.

In the North Atlantic onshore regions, granite related molybdenite mineralization is documented throughout the UK, Irish and Newfoundland Caledonian-Appalachian Orogen (**Lynch *et al.*, 2009; Feely *et al.*, 2010; Holdsworth *et al.*, 2015**). The broad timing (and fluid characteristics) of the Mo mineralization in the UK sector *e.g.* Loch Shin and Grudie Granite veins (c. 428 Ma; **Holdsworth *et al.*, 2015**) is similar to that of the Ballachulish and Kilmelford igneous complexes, including the Lagalochan porphyry Cu–Mo system (c. 433Ma–426 Ma; **Conliffe *et al.*, 2010**), and predates that of the Etive Igneous Complex (c. 415 Ma; **Porter and Selby, 2010**), and Shap granite (c. 405 Ma; **Selby *et al.*, 2008**). Mo mineralization in the Ackley granite (Newfoundland sector) occurred ~380Ma (**Lynch *et al.*, 2009**). Granite-related Mo mineralization in the GGC of the Irish sector of the Caledonian–Appalachian Orogen spanned ~40Ma from ~ 425 – 380 Ma and overlaps with the range of ages above (**Feely *et al.*, 2010**).

Jenkin *et al.* (1997) argued that the hydrothermal fluorite veins in the GGC represent late-Triassic mineralisation and forms part of a broader North Atlantic-European

Triassic-Jurassic hydrothermal mineralisation province identified by **Mitchell and Halliday (1976)**. This model involved the rifting of the N Atlantic triggering crustal thinning and subsidence of continental crust and initiating hydrothermal activity at the margins of Mesozoic basins thus facilitating hydrothermal vein fluorite mineralisation in for example, granite basement rocks like the GGC **(Mitchell and Halliday, 1976; Halliday and Mitchell 1984; O'Connor *et al.*, 1993)**.

Acknowledgements

Jimi and Stephen Larkin, Larkin's Granite Quarry, Shannaphaesteen, Co. Galway, Ireland to access to the quarry. MF acknowledges several constructive discussions, with Professor Bernard Leake, Cardiff University, UK, on matters relating to the Galway Granite Complex. Thanks to Drew Coleman and Josh Rosera (University of North Carolina, Chapel Hill, NC, US) for facilitating and assisting in the lab work and analyses for zircon geochronology. DS acknowledges the technical support of Geoff Nowell, Antonia Hoffman, and Chris Ottley, and the Total Endowment Fund and Dida Scholarship of CUG Wuhan.

552 **References**

553 **Ayuso, R.A., 1999.** Geochemical and metallogenic contrasts in Palaeozoic granitic
554 rocks of the northern New England Appalachians. In: Norumbega Fault system of
555 the northern Appalachians (ed. Ludman, A and West, D.P.) *GSA Spec paper* 331,
556 155-166, Boulder, CO, USA.

557 **Bakker R. J., 2003.** Clathrates: computer programs to calculate fluid inclusion V-X
558 properties using clathrate melting temperatures. *Computers and Geosciences*
559 23(1): 1-18.

560 **Bodnar, R.J., 1993.** Revised equation and table for determining the freezing point
561 depression of H_2O-NaCl solutions. *Geochimica et Cosmochimica Acta*, **57**, 683-684.

562 **Bodnar, R.J., 2003.** Introduction to fluid inclusions. In I. Samson, A. Anderson, & D.
563 Marshall, eds. Fluid Inclusions: Analysis and Interpretation. *Mineralogical*
564 *Association of Canada*, Short Course 32, 1-8.

565 **Bowring, J.F., McLean, N.M., Bowring, S.A., 2011**. Engineering cyber
566 infrastructure for U-Pb geochronology: Tripoli and U-Pb Redox. *Geochemistry,*
567 *Geophysics, Geosystems*, 12, 6, Q0AA19.

568 **Buchwaldt, R., Kroner, A., Toulkeredes, T., Todt, W., Feely, M., 2001.**
569 Geochronology and Nd-Sr systematics of Late Caledonian granites in western
570 Ireland: new implications for the Caledonian orogeny. *Geological Society of*
571 *America Abstracts with Programs* 33, 1, A32.

572 **Buret, Y., Wotzlaw, J.F., Roozen, S., Guillong, M., von Quadt, A., Heinrich,**
573 **C.A., 2017**. Zircon petrochronological evidence for a plutonicvolcanic
574 connection in porphyry copper deposits. *Geology*, 45(7), 623-626.

575 **Canals, A., Cardellach, E., 1993.** Strontium and sulphur isotope geochemistry of
576 low-temperature barite-fluorite veins of the Catalonian Coastal Ranges (NE

577 Spain): a fluid mixing model and age contraints. *Chemical Geology*, 104, 269-
578 280.

579 **Chelle-Michou, C., Chiaradia, M., Ovtcharova, M., Ulianov, A., Wotzlaw, J.F.**
580 **2014**. Zircon petrochronology reveals the temporal link between porphyry
581 systems and the magmatic evolution of their hidden plutonic roots (the Eocene
582 Coroccohuayco deposit, Peru). *Lithos*, **198-199**, 129-140.

583 **Chesley, J.T., Halliday, A.N., Snee, L.W., Mezger, K., Shepherd, T., Scrivener,**
584 **R.C., 1993.** Thermochronology of the Cornubian batholith in southwest England:
585 Implications for pluton emplacement and protracted hydrothermal mineralization.
586 *Geochimica et Cosmochimica Acta*, 57(8):1817-1835.

587 **Conliffe, J., Blamey, N.F., Feely, M., Parnell, J. and Ryder, A.G., 2010.**
588 Hydrocarbon migration in the Porcupine Basin, offshore Ireland: evidence from
589 fluid inclusion studies. Petroleum Geoscience, 16, 67-76.

590 **Conliffe, J. and Feely M. 2010.** Fluid inclusions in Irish granite quartz: Monitors of
591 fluids trapped in the onshore Irish Massif. Earth and Environmental Science
592 *Transactions of the Royal Society of Edinburgh*, 101(01):53-66.

593 **Conliffe, J., Selby, D., Porter, S.J. & Feely, M. 2010.** Re–Os molybdenite dates
594 from the Ballachulish and Kilmelford Igneous complexes (Scottish Highlands):
595 Age contraints for late Caledonian magmatism. *Journal of the Geological*
596 *Society, London*, **167**, 297–302.

597 **Costanzo, A., Feely, M. 2019**. A review of important gem material from Connemara,
598 western Ireland. *Proceeding of the 36th International Gemmological Conference*,
599 Nantes, France, 58-60.

600 **Derham, J.M**., **1986**. Structural control of sulphide mineralization at Mace Head, Co.
601 Galway. In: Andrew C. J., Crowe R. W. A., Finlay S., Pennell W. M., Pyne J. F.

(eds) Geology and genesis of mineral deposits in Ireland. *Irish Association Economic Geology*, 187-193

Derham J.M., Feely, M., 1988. A K-feldspar breccia from the Mo-Cu stockwork deposit in the Galway Granite, west of Ireland. *Journal of Geological Society of London* 145, 661-667

Dewey, J., Ryan, P.D., 2016. Connemara: its position and role in the Grampian Orogeny. *Canadian Journal of Earth Sciences.* 53, 1246-1257

Dewey, J.F., Strachan, R.A., 2003. Changing Silurian–Devonian relative plate motion in the Caledonides: sinistral transpression to sinistral transtension. *Journal of the Geological Society*, 160, 219-229.

Draut, A.E., Clift, P.D., 2002. The origin and significance of the Delaney Dome Formation, Connemara, Ireland. *Journal of the Geological Society* **159** (1), 95-103.

Feely, M., Coleman, D.S., Baxter, S., Miller, B., 2003. U-Pb zircon geochronology of the Galway Granite, Connemara, Ireland: implications for the timing of late Caledonian tectonic and magmatic events and for correlations with Acadian plutonism in New England. *Atlantic Geology* 39, 175-184.

Feely, M., Costanzo, A., Lindner, F., George, J., Parnell, J., Bowden, S., Mas'ud Baba and Owens, P. 2017. Quartz-Amethyst Hosted Hydrocarbon-Bearing Fluid Inclusions from the Green Ridge Breccia in the Snoqualmie Granite, North Cascades, WA, USA. *Minerals*, 7, 174.

Feely, M., Gaynor, S., Venugopal, N., Hunt, J., Coleman, D.S., 2018. New U-Pb zircon ages for the Inish Granite Pluton, Galway Granite Complex, Connemara, Western Ireland. *Irish Journal of Earth Sciences, 36(1),* 1-7.

Feely, M., Hoegelsberger H., 1991. Preliminary fluid inclusion studies of the Mace

627 Head Mo-Cu deposit in the Galway Granite, *Irish Journal of Earth Sciences*, 11,
628 1-10.

629 **Feely, M., Leake, B.E., Baxter, S., Hunt, J., Mohr, P., 2006.** A Geological Guide to
630 the Granites of the Galway Batholith, Connemara, western Ireland. Publisher
631 *Geological Survey of Ireland*, Dublin. ISBN 1-899702-56-3

632 **Feely, M., Selby, D., Conliffe, P., Judge, M., 2007.** Re-Os geochronology and fluid
633 inclusion microthermometry of molybdenite mineralization in late-Caledonian
634 Omey Granite, Western Ireland. *Applied Earth Science* 116, 3, 143-149.

635 **Feely, M., Selby, D., Hunt, J., Conliffe, P., 2010.** Long-lived granite-related
636 molybdenite mineralization at Connemara, western Irish Caledonides. *Geological*
637 *Magazine*, 147, 6, 886-894.

638 **Ferguson, C.C., Al-Ameen, S.I. 1985.** Muscovite breakdown and corundum growth
639 at anomalously low f H_2O: a study of contact metamorphism and convective fluid
640 movement around the Omey granite, Connemara, western Ireland. *Mineralogical*
641 *Magazine*, **49**, 505-515.

642 **Friedrich, A.M., Bowring, S.A., Martin, M.W., Hodges, K.V., 1999a.** Short-lived
643 continental magmatic arc at Connemara, western Irish Caledonides: Implications
644 for the age of the Grampian orogeny. *Geology*, **27,** 27-30.

645 **Friedrich, A.M., Hodges, K.V., Bowring, S.A., Martin, M., 1999b.**
646 Geochronological constraints on the magmatic, metamorphic and thermal
647 evolution of the Connemara Caledonides, western Ireland. *Journal of Geological*
648 *Society of London*, **156**, 1217-30.

649 **Friedrich, A.M., Hodges, K.V., 2016.** Geological significance of 40Ar/39Ar mica
650 dates across a mid-crustal continental plate margin, Connemara (Grampian

orogeny, Irish Caledonides), and implications for the evolution of lithospheric collisions. *Canadian Journal of Earth Sciences*, 53, 1258-1278.

Gallagher, V., Feely, M., Hoegelsberger, H., Jenkin, G.R.T., Fallick, A.E., 1992. Geological, Fluid inclusion and stable isotope studies of Mo mineralization, Galway Granite, Ireland. *Mineralium Deposita*, 27, 314-325

Gaynor, S.P., Rosera, J.M., Coleman, D.S., 2019. Intrusive history of the Oligocene Questa porphyry molybdenum deposit, New Mexico. *Geosphere*. 15(2), 548-575.

Halliday A.N., Mitchell, J.G., 1984. K-Ar ages of clay-size concentrates from the mineralisation of the Pedroches Batholith, Spain, and evidence for Mesozoic hydrothermal activity associated with the breakup of Pangea. *Earth and Planetary Science Letters*. 68, 229-239.

Holdsworth, B., Dempsey, E.D., Selby, D., Darling, J., Feely, M., Costanzo, A., Strachan, R., Waters, P., Finlay A., Porter, S.J., 2015. Silurian to Devonian magmatism, molybdenite mineralization, regional exhumation and brittle strike-slip deformation along the Loch Shin Line, NW Scotland. *Journal of Geological Society London*, **172**, 748-762.

Holdsworth, R.E., McCaffrey, K.J.W., Dempsey, E., Roberts, N.M.W., Hardman, K., Morton, A., Feely, M., Hunt, J., Conway, A., Robertson, A., 2019. Natural fracture propping and earthquake-induced oil migration in fractured basement reservoirs. *Geology*, 47(8), 700-704.

Jaffey, A.H., Flynn, K.F., Glendenin, L.E., Bentley, W.C., Essling, A.M., 1971. Precision measurement of half-lives and specific activities of ^{235}U and ^{238}U. *Physical Review*, 4, 1889–1906.

Jenkin, G.R.T., Mohr, P., Mitchell, J.G., Fallick, A.E., 1998. Carboniferous dykes as monitors of post-Caledonian fluid events in West Connacht, Ireland. *Transactions of the Royal Society of Edinburgh, Earth Sciences*, 89, 225-243.

Jenkin, G.R.T., O,Reilly, C., Feely, M., Fallick, A.E., 1997. The geometry of mixing of surface and basinal fluids in the Galway Granite, Connemara, Western Ireland. In: Hendry, J., Carey, P., Parnell, P., Ruffell, A. & Worden, R. (eds), Proceedings of Geofluids II '97, (Queens University Belfast) Conference Volume ISBN 1-897799-83-7. 374-377.

Krogh, T.E., 1973. A low-contamination method for hydrothermal decomposition of zircon and extraction of U and Pb for isotopic age determinations. *Geochimica et Cosmochimica Acta*, 37, 385-494.

Lawley, C.J.M., Selby, D. 2012. Re-Os Geochronology of Quartz Enclosed Ultra-fine Molybdenite: Implications for Ore Geochronology, *Economic Geology*, 107, 1499-1506.

Leake, B.E., 1989. The metagabbros, orthogneisses and paragneisses of the Connemara Complex, western Ireland. *Journal of Geological Society of London* 146, 574-96.

Leake, B.E., 2006. Mechanism of emplacement and crystallisation history of the northern margin and centre of the Galway Granite, western Ireland. *Transactions of the Royal Society of Edinburgh: Earth Sciences*, 97, 1-23.

Leake, B.E., Singh, D., 1986. The Delaney Dome Formation, Connemara, W. Ireland, and the geochemical distinction of ortho- and para-quartzofeldspathic rocks. *Mineralogical Magazine*, 50 (356), 205-215.

Leake, B.E., Tanner, P.W.G., 1994. The geology of the Dalradian and associated rocks of Connemara, Western Ireland. *Royal Irish Academy*, Dublin. pp. 96. ISBN 1-874045-18-6.

Lees, A., Feely, M., 2016. The Connemara eastern boundary fault: a review and assessment using new evidence. *Irish Journal of Earth Sciences*, 34, 1-25.

Lees, A., Feely, M., 2017. The Connemara Eastern Boundary Fault: A correction. *Irish Journal of Earth Sciences, 35*, 55-56

Li, Y., Selby, D., Condon, D., Tapster, S., 2017. Cyclic magmatic-hydrothermal evolution in porphyry systems: High-precision U-Pb and Re-Os geochronology constraints from the Tibetan Qulong porphyry Cu-Mo deposit. *Economic Geology*, 112, 1419-1440.

Lynch, E.P., Selby, D., Feely, M., Wilton, D.H.C 2009. New constraints on the timing of molybdenite mineralization in the Devonian Ackley Granite suite, south-eastern Newfoundland: preliminary results of Re–Os geochronology. *Current Research, Newfoundland and Labrador Department of Natural Resources Geological Survey*, Report 09-1, 1-10.

MacDonald, A.J., Spooner, E.T.C., 1981. Calibration of a Linkam TH 600 programmable heating-cooling stage for microthermometric examination of fluid inclusions. *Economic Geology*, 74, 1249-1258.

Markey, R., Stein, H., Morgan, J., 1998. Highly precise Re–Os dating for molybdenite using alkaline fusion and NTIMS. *Talanta* **45**, 935–46.

Mattinson, J.M., 2005. Zircon U-Pb chemical abrasion ("CA-TIMS") method: Combined annealing and multi-step partial dissolution analysis for improved precision and accuracy of zircon ages. *Chemical Geology*, 220(1-2), 47-66.

Max, M.D., Talbot, V., 1986. Molybdenum concentrations in the western end of the

722 Galway Granite and their structural setting. In Geology and genesis of mineral
723 deposits in Ireland (eds C.J. Andrews, R.W.A. Crowe, S. Finlay, W.M. Pennell &
724 J. Pyne), *Irish Association for Economic Geology*, 177-85.
725 **McCaffrey, K., Johnson, D., Feely, M., 1993**. Use of fractal statistics in the analysis
726 of Mo-Cu mineralisation at Mace Head, County Galway. *Irish Journal of Earth*
727 *Sciences* 12, 139-148.
728 **McCaffrey, K.J.W., Lonergan, L., Wilkinson, J.J., 1999.** Fractures, fluid flow and
729 mineralization. *Geological Society Special Publication*, No. 155.
730 **McKie, D., Burke, K., 1955.** The geology of the islands of south Connemara.
731 *Geological Magazine*, 92: 487-498.
732 **McLean, N.M., Bowring, J.F., Bowring, S.A., 2011**. An algorithm for U-Pb isotope
733 dilution data reduction and uncertainty propagation. *Geochemistry, Geophysics,*
734 *Geosystems*, 12, Q0AA18.
735 **Menuge. J.F., Feely. M., O'Reilly, C. 1997**. Origin and granite alteration effects of
736 hydrothermal fluid: isotopic evidence from fluorite veins, Co. Galway, Ireland.
737 *Mineralium Deposita*. 32, 34-43
738 **Mitchell, J.G., Halliday, A.N., 1976.** Extent of Triassic/Jurassic hydrotrhermal ore
739 deposits on the North Atlantic margins. Transactions of the Institution of Mining
740 & Metallurgy, B85, 159-161.
741 **Mohr, P., 2004.** Late magmatism of the Galway Granite batholith: II. composite
742 dolerite-rhyolite dikes. *Irish Journal of Earth Sciences*, 22, 15-32.
743 **Mohr, P., 2018** *Irish Journal of Earth Sciences*38-42.**Mundil, R., Ludwig, K.R.,**
744 **Metcalf, I., Renne, P.R., 2004**. Age and timing of the Permian mass extinctions:
745 U/Pb dating of closed-system zircons. *Science*, 305, 669-673.

Munoz, M., Boyce, A.J., Courjault-Rade, P., Fallick, A.E., Tollon, F., 1994. Multi-stage fluid incursion in the Palaeozoic basement-hosted Saint-Salvy ore deposit (NW Montagne Noire, southern France). *Applied Geochemistry*, 9(6), 609-626.

O'Connor, P.J., Hogelsberger, H., Feely, M., Rex, D.C., 1993. Fluid inclusion studies, rare-earth element chemistry and age of hydrothermal fluorite mineralization in Western Ireland - a link with continental rifting? *In Transactions of the Institute of Mining & Metallurgy*, 102b (9/12), 141-148. *London: E. & F.N. Spon 1893-1965.*

O'Raghallaigh, C., Feely, M., MCardle, P., MacDermot, C., Geoghegan, M., Keary, R. 1997. *Mineral localities in the Galway Bay Area, Geological Survey of Ireland*, Report Series, RS97/1 (Mineral Resources), 70 pp.

O'Reilly, C., Jenkin, G.R.T., Feely, M., Alderton, D.H.M., Fallick, A.E., 1997. A fluid inclusion and stable isotope study of 200 Ma of fluid evolution in the Galway Granite, Connemara, Ireland. *Contributions to Mineralogy & Petrology*, 129(2-3), 120-142.

Ovtcharova, M., Goudemand, N., Hammer, O., Gudoun, K., Cordey, F., Galfetti, T., Schaltegger, U., Bucher, H., 2015. Developing a strategy for accurate definition of a geological boundary through radio-isotope and biochronological dating: The Early-Middle Triassic boundary (South China). *Earth-Science Reviews*, 146, 65-76.

Parnell, J., 1988. Migration of biogenic hydrocarbons into granites: A review of hydrocarbons in British plutons. *Marine and Petroleum Geology*, 5, 385-396.

Parrish, R.P., 1987. An improved micro-capsule for zircon dissolution in U-Pb geochronology. *Chemical Geology*, 66, 99-192.

Parrish, R.P., Krogh, T.E., 1987. Synthesis and purification of 205Pb for U-Pb geochronology. *Chemical Geology*, 66, 103-110.

Petford, N., McCaffrey, K., 2003. In Hydrocarbons in Crystalline Rocks, Geological Society Special Publication No.214. Hydrocarbons in crystalline rocks: an introduction. *The Geological Society London*, 1-6.

Plant, J.A. 1986. Models for granites and their mineralising systems in British and Irish Caledonides, in Geology and genesis of mineral deposits in Ireland, (ed. C. J. Andrews *et al*.), 121–156; Dublin, *Irish Association for Economic Geology*

Porter, S.J. & Selby, D. 2010. Rhenium–osmium (Re–Os) molybdenite systematics and geochronology of the Cruachan Granite skarn mineralization, Etive Complex: Implications for emplacement chronology. *Scottish Journal of Geology*, **46**, 17–21.

Pracht, M., Lees, A., Leake, B.E., Feely, M., Long, B.C., Morris, J., McConnell, B., 2004. Geology of Galway Bay: A geological description to accompany the Bedrock Geology 1:100,000 Scale Map Series, Sheet 14, Galway Bay. *Geological Survey of Ireland*, Dublin.

Roedder, E., 1984. Fluid inclusions. Reviews in Mineralogy. Mineralogical Society of America, **12**, 664 pp.

Samperton, K.M., Schoene, B., Cottle, J.M., Keller, C.B., Crowley, J.L., Schmitz, M.D., 2015. Magma emplacement, differentiation and cooling in the middle crust: Integrated zircon geochronological-geochemical constraints from the Bergell intrusion, Central Alps. *Chemical Geology*, 417, 322-340.

Schaltegger, U., Brack, P., Ovtcharova, M., Peytcheva, I., Schoene, B., Stracke, A., Marocchi, M., Bargossi, G.M., 2009. Zircon and titanite recording 1.5million years of magma accretion, crystallization and initial cooling in a

composite pluton (southern Adamello batholith, northern Italy). *Earth and Planetary Science Letters*, 286(1-2), 208-218.

Schoene, B., 2014. U-Th-Pb Geochronology. *In* H.D. Holland & K.K. Turekian (Eds.), Treatise on Geochemistry, 341-378. Oxford, England: Elsevier.

Selby, D., Creaser, R.A., Feely, M., 2004 Accurate Re-Os molybdenite dates from the Galway Granite, Ireland. A critical comment to: Disturbance of the Re-Os chronometer of molybdenites from the late-Caledonian Galway Granite, Ireland, by hydrothermal fluid circulation. *Geochemical Journal* 38, 291-294.

Selby, D., Creaser, R.A., 2001. Re–Os geochronology and systematics in molybdenum from the Endako porphyry molybdenum deposit, British Columbia, Canada. *Economic Geology* **96**, 197–204.

Selby, D., Creaser, R.A., 2004. Macroscale NTIMS and microscale LA-MC-ICP-MS Re–Os isotopic analysis of molybdenite: Testing spatial restriction for reliable Re– Os age determinations, and implications for the decoupling of Re and Os within molybdenite. *Geochimica et Cosmochimica Acta* **68**, 3897–908.

Selby, D., Creaser, R.A., Stein, H.J., Markey, R.J., Hannah, J.L., 2007. Assessment of the 187Re decay constant accuracy and precision: cross calibration of the 187Re–187Os molybdenite and U-Pb zircon chronometers. *Geochimica et Cosmochimica Acta* **71**, 1999–2013.

Selby, D., Conliffe, J., Crowley, Q. & Feely, M. 2008. Geochronology (Re–Os and U–Pb) and fluid inclusion studies of molybdenite mineralisation associated with the Shap, Skiddaw and Weardale granites, UK. *Transactions of the Institute of Mining and Metallurgy, Section B*, **117**, 11–28.

Shepherd, T.J., Rankin, A.H. and Alderton, D.H.M., 1985. A practical guide to fluid inclusion studies. Glasgow and London, Blackie, Glasgow.

Shukla, M.K., Sharma, A., 2018. A brief review in breccia: its contrasting origin and diagnostic signatures. *Solid Earth Sciences* **3**, 50–59.

Smoliar, M.I., Walker, R.J., Morgan, J.W., 1996. Re-Os isotope constraints on the age of Group IIA, IIIA, IVA and IVB iron meteorites. *Science* **271**, 1099–1102.

Steele-MacInnis, M., Bodnar, R.J., Naden, J., 2011. Numerical model to determine the composition of H_2O–NaCl–$CaCl_2$ fluid inclusions based on microthermometric and microanalytical data. *Geochimica et Cosmochimica Acta*, 75 (1). 21-40.

Steiger, R.H., Jager, E., **1977**. Subcommission of geochronology; convention on the use of decay constants in geo- and cosmo-chemistry. *Earth Planetary Scientific Letters*, 36(3), 359-362.

Stein, H.J., Markey, R.J., Morgan, J.W., 1997. Highly precise and accurate Re–Os ages for molybdenite from the east Qinling molybdenum, Shaanxi province, China. *Economic Geology* **92**, 827–35.

Streckeisen, A., 1967. Classification and nomenclature of igneous rocks. Final report of an inquiry. *N. Jahrb. Miner. Abh.*, 107, 144-240.

Trice R., 2014. Basement exploration, West of Shetlands: progress in opening a new play on the UKCS *in* Hydrocarbon Exploration to Exploitation West of Shetlands, *Geological Society, London, Special Publications, eds* Cannon S.J.C., Ellis D. First published online February 28, 397.

von Quadt, A., Erni, M., Marinek, K., Moll, M., Peytcheva, I., Heinrich, C.A., 2011. Zircon crystallization and the lifetimes of ore-forming magmatic-hydrothermal systems. *Geology*, 39(8), 731-734.

Whalen, J.B. 1993. Geology, petrography and geochemistry of Appalachian granites in New Brunswick and Gaspesie, Quebec, *Geol. Surv. Can. Bull.*, 436, 130.

Widmann, P., Davies, J.H.F.L., Schaltegger, U., 2019. Calibrating chemical abrasion: Its effects on zircon crystal structure, chemical composition and U-Pb age. *Chemical Geology*, 511, 1-10.

Williams D.M., Armstrong H.A., Harper D.A.T., 1988. The age of the South Connemara Group, Ireland, and its relationship to the Southern Uplands Zone of Scotland and Ireland. *Scottish J. Geol.* 23: 279-287

Wotzlaw, J.F., Schaltegger, U., Frick, D.A., Dungan, M.A., Gerdes, A., Gunther, D., 2013. Tracking the evolution of large-volume silicic magma reservoirs from assembly to supereruption. *Geology*, 41, 867-870.

Figure Captions

Figure 1. Geological map of the Galway Granite Complex (GGC) showing the spatial disribution of major lithologies and structures (adapted from **Feely *et al.*, 2006 and Leake 2006**). The early plutons are: Roundstone granite (R), Inish granite (I), Omey granite (O), Letterfrack (L). D is the Delaney Dome Fm. comprising lower Ordovician metavolcanic rocks. Quarry Locations 1: Larkin's Quarry Shannpheasteen; 2: Costelloe Murvey Granite Quarry. Location of sample GBM is also shown.

Figure 2. A composite map of Larkin's Quarry derived using a combination of aerial photography and mapped geological features. Samples used in this study are: quarry granodiorite (LQ-1), molybdenite-bearing quartz vein (LQ-2) and the main fluorite vein (LQ-3).

Figure 3. A selection of field photographs from Larkin's Quarry. a) Quarry granodiorite showing vertical-dipping biotite fabric. b) The molybdenite-bearing quartz vein. c) Feldspar porphyry dike cut by millimetric scale veinlets of fluorite. d) Deeply weathered dolerite dyke exposed at south-eastern end of the quarry. e) The main fluorite vein with insets highlighting the brecciated nature of the host quarry granodiorite (bottom left) and the exceptional quality of the fluorite crystals in the anastomosing fluorite vugs (top right).

879 **Figure 4.** Gem fluorite crystals from Larkin's Quarry. The bicolour crystal (~2cm in
880 width, centre of the image) is a cube and octahedron combination. Purple-coloured
881 octahedral faces contrast with the colourless transparent cubic faces.
882
883 **Figure 5.** a) U-Pb concordia plot of zircons analysed from the quarry granodiorite
884 sample (LQ-1) and b) Weighted mean plot of U-Pb zircon ages for LQ-1.
885
886 **Figure 6.** A selection of photomicrographs showing primary two-phase
887 (liquid+vapour; L>V) fluid inclusions hosted by a) molybdenite-bearing vein quartz
888 (GBM), b) molybdenite-bearing vein quartz (LQ-2) and c) vein fluorite (LQ-3).
889 Homogenisation temperatures (T_H) and salinities (eq.wt.%NaCl) for some of the FIs
890 are also shown.
891
892 **Figure 7.** Bivariate plots of temperature of homogenisation (T_H) and salinity (eq.
893 wt.% NaCl) showing fields of the three main fluid types after **O'Reilly *et al.*, (1997)**.
894 The aqueous-carbonic fluids are associated with molybdenite mineralization. The
895 lower-T aqueous fluids of low to moderate salinity formed from mixing between late
896 magmatic and meteoric fluids. The third group represents late Triassic hydrothermal
897 fluids with higher salinity and lower temperature. The data from this study are plotted
898 to show the similarities between the aqueous fluids hosted by the molybdenite-bearing
899 vein quartz (LQ-2 and GBM) and the vein fluorite (LQ-3).
900
901 **Figure 8.** A comparative plot of modelled fluid inclusion compositions from vein
902 fluorite in the Costelloe Murvey Granite quarry (COS-2 and COS-4; n=19)
903 (O'Connor *et al.,* 1993) and from the Larkin's Granodiorite Quarry at

Shannapheasteen (LQ-3; n=32). The grey field is based upon fluid compositions recorded by Conliffe and Feely, 2010 from Irish granite basement.

Figure 9: Pressure-temperature space showing isochores for primary Type 1 FIs from molybdenite-bearing vein quartz (LQ-2 and GBM) and fluorite veins (LQ-3, COS-2 and COS-4). Isochores LQ-2 and GBM are constrained by pressure estimates from Gallagher *et al.* (1992). Shaded P–T fields for Mo-mineralization in the Omey pluton (Feely *et al.*, 2007) and the Carna pluton (Gallagher *et al.*, 1992) are also shown. The ages shown are Re-Os ages for magmatic molybdenite mineralization in the GGC. The vein fluorite isochores LQ-3, COS-2 and COS-4 are constrained by an assumed lithostatic pressure of 1 kbar equivalent to a sedimentary cover of ~3.5km. The parameters used for the construction of the isochores are shown on the top corner of the P-T space diagram.

Table 1. U-Pb Zircon data for mineralized granite

Table 2. Re-Os molybdenite data from sample LQ-2.

Table 3: Fluid inclusion types observed in the molybdenite-bearing vein quartz samples (LQ-2 and GBM) and in the vein fluorite sample (LQ-3). Qualitative assessment of fluid inclusion abundance is: X - low to medium abundance; XX - high abundance.

Table 4: Microthermometric data for primary Type 1 inclusions in the two molybdenite-bearing vein quartz (GBM and LQ-2) and vein fluorite (LQ-3). T_{FM}:

929 temperature of first ice melting; T_{Mhyd}: temperature of hydrohalite melting; T_{LM}:
930 temperature of last ice melting; T_H: temperature of homogenization; eq. wt.%:
931 equivalent weight per cent; (-) = not observed. The salinity (NaCl +$CaCl_2$) was
932 calculated using the model of Steele-MacInnis, *et al.*, 2011.

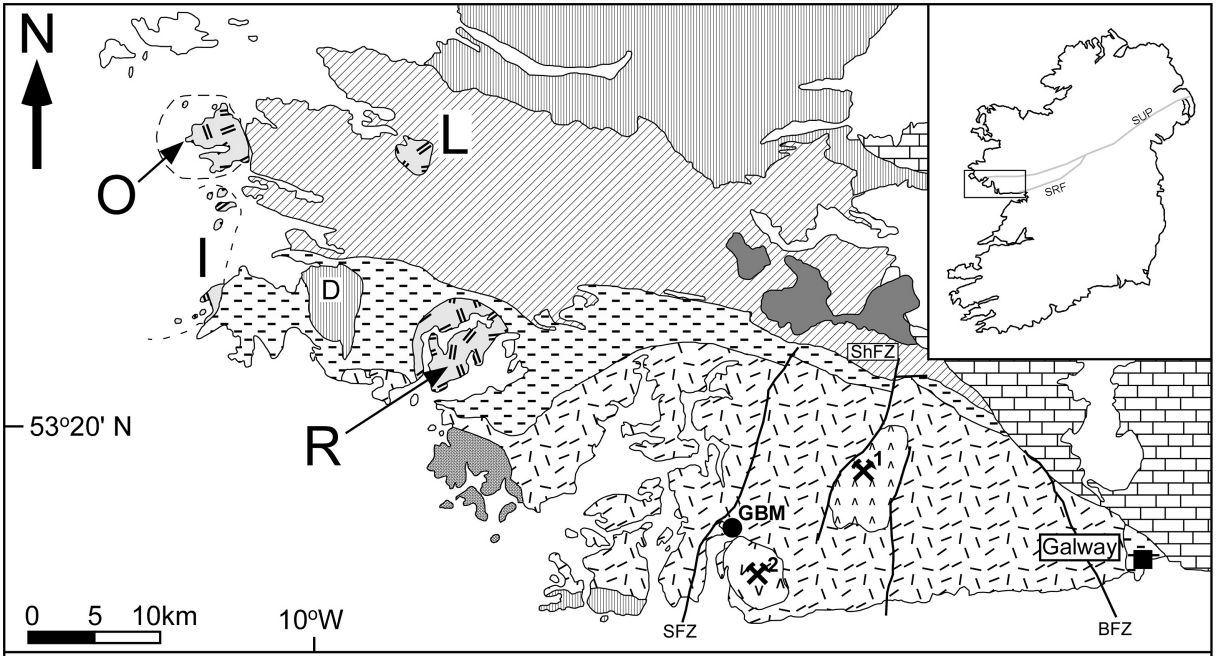

Costelloe Murvey Granite

Shannapheasteen Granite

Kilkieran Pluton

Carna Pluton

Early Plutons

SUP: Southern Uplands Fault

SRF: Skerd Rocks Fault

Quarry

Carboniferous Limestone

Silurian and Ordovician Sediments

Oughterard Granite

Metagabbro-Gneiss Suite

Dalradian Metasediments

ShFZ: Shannapheasteen Fault Zone

SFZ: Shannawona Fault Zone

BFZ: Barna Fault Zone

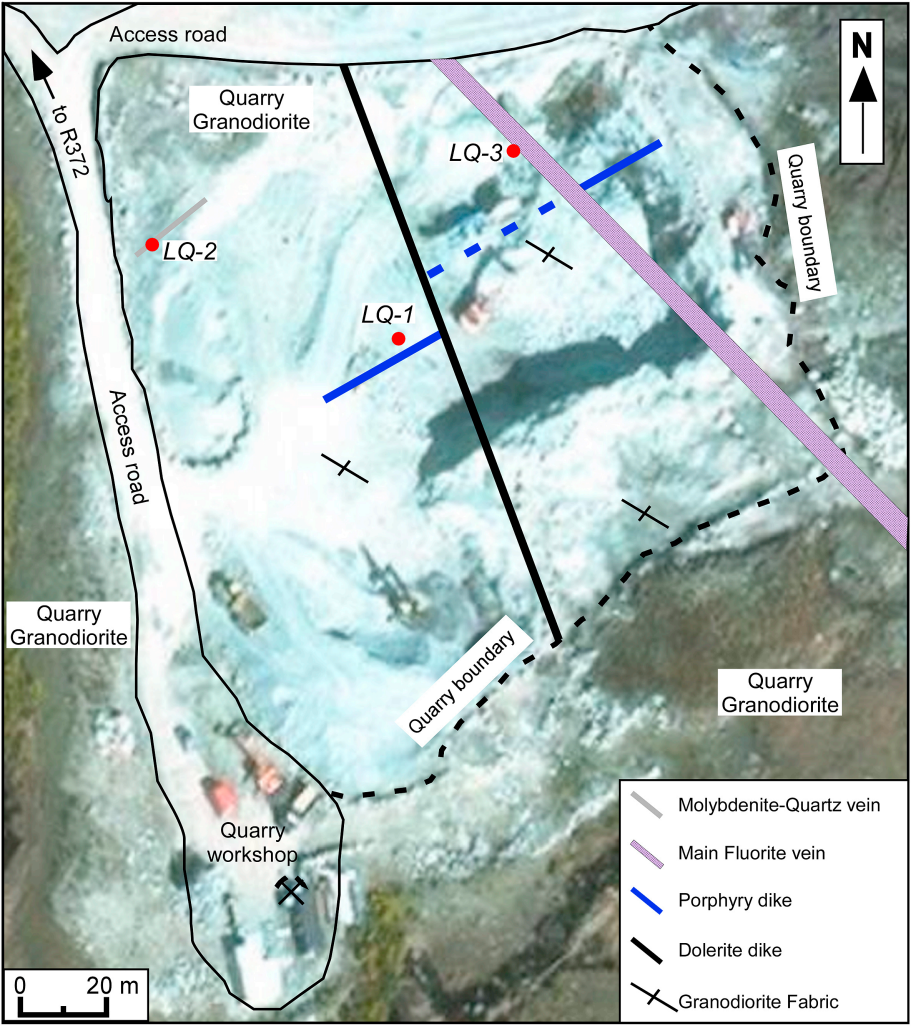
Access road
to R372
Quarry Granodiorite
LQ-3
LQ-2
LQ-1
Quarry boundary
N
Access road
Quarry Granodiorite
Quarry boundary
Quarry Granodiorite
Quarry workshop
0
20 m
Molybdenite-Quartz vein
Main Fluorite vein
Porphyry dike
Dolerite dike
Granodiorite Fabric

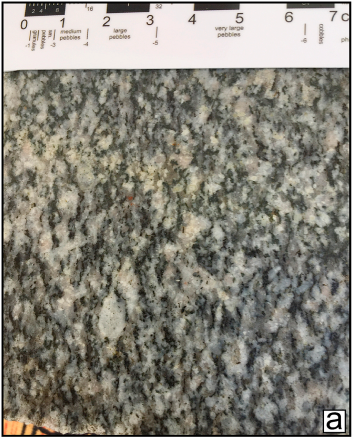
0
1
2
3
4
5
6
7
medium pebbles
large pebbles
very large pebbles
a


PERMANENT
b


c


d


e

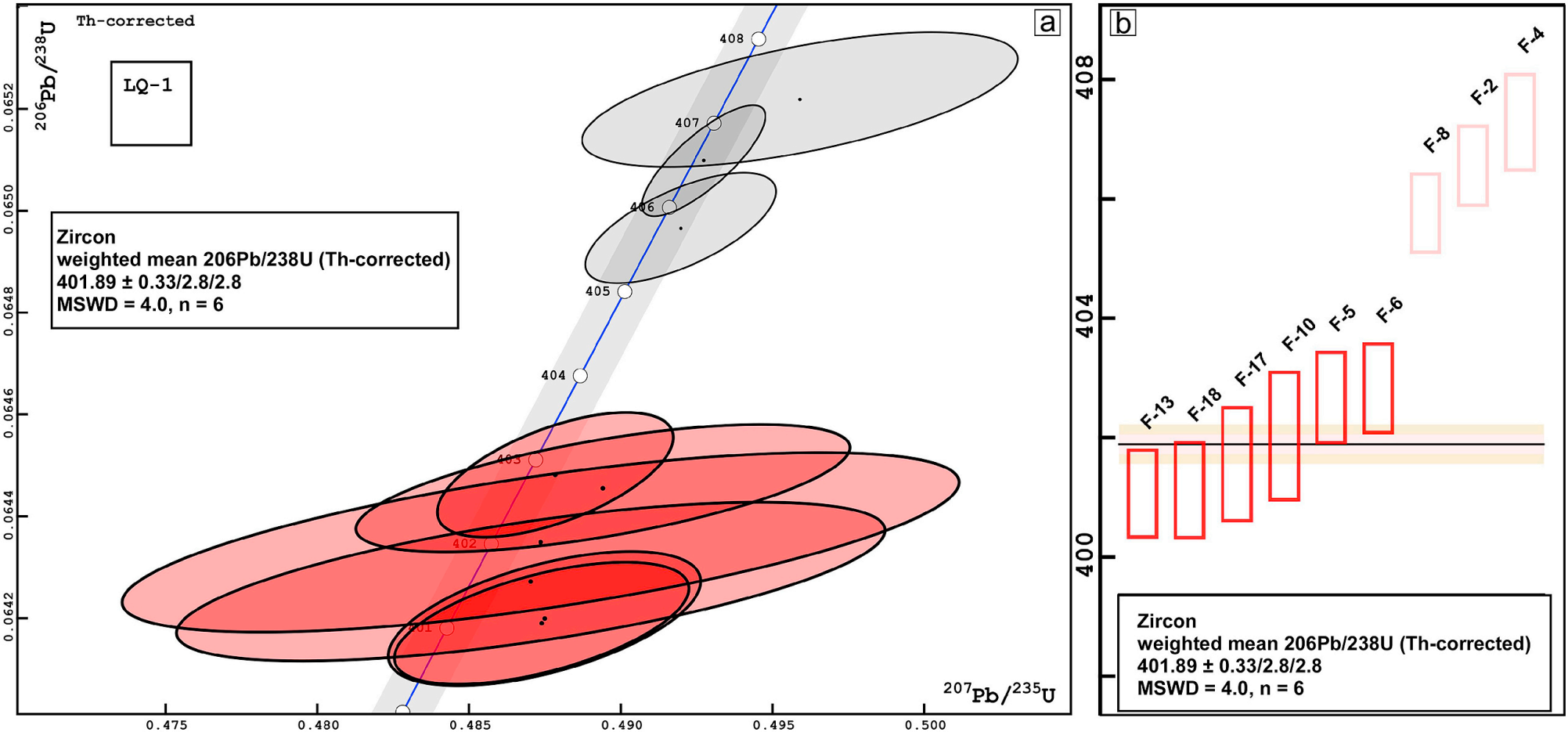
Th-corrected
LQ-1
a
$^{206}Pb/^{238}U$
$^{207}Pb/^{235}U$
0.0652
0.0650
0.0648
0.0646
0.0644
0.0642
0.475
0.480
0.485
0.490
0.495
0.500
408
407
406
405
404
403
402
401
Zircon
weighted mean 206Pb/238U (Th-corrected)
401.89 ± 0.33/2.8/2.8
MSWD = 4.0, n = 6
b
408
404
400
F-4
F-2
F-8
F-6
F-5
F-10
F-17
F-18
F-13
Zircon
weighted mean 206Pb/238U (Th-corrected)
401.89 ± 0.33/2.8/2.8
MSWD = 4.0, n = 6

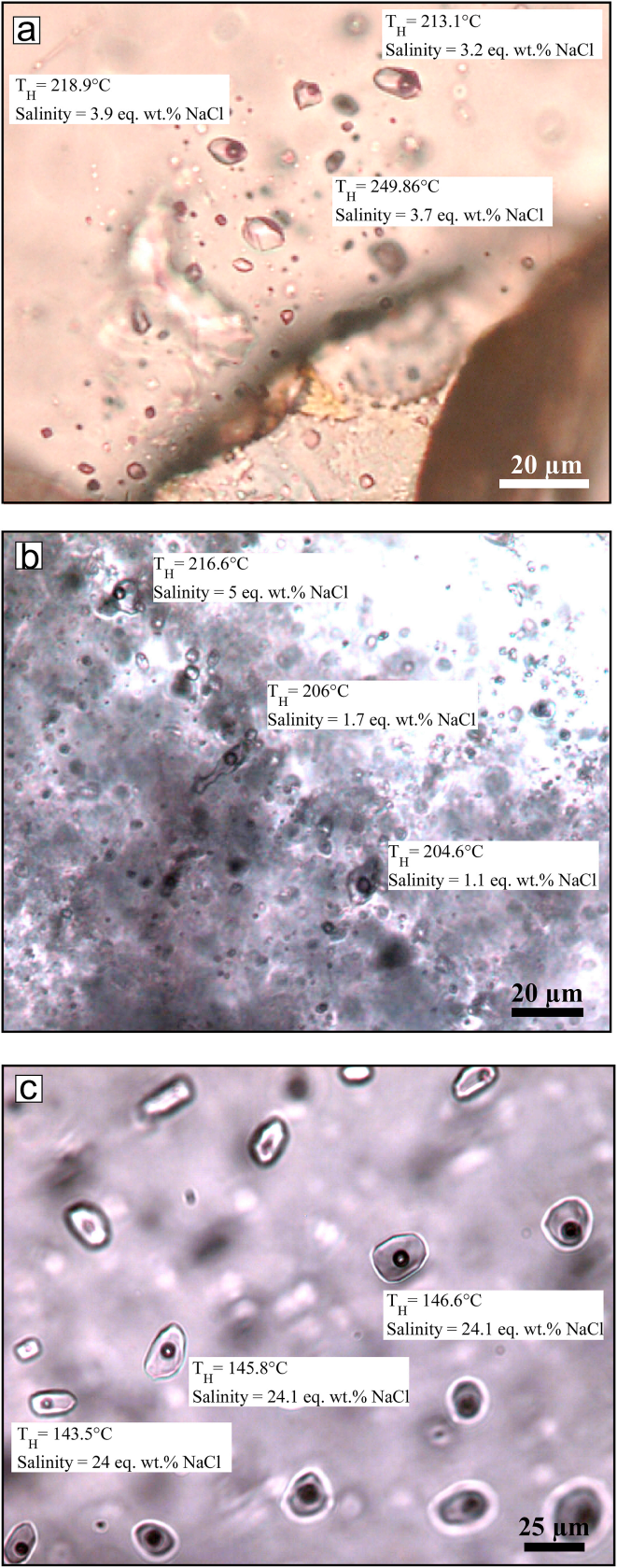
a
T_H = 213.1°C
Salinity = 3.2 eq. wt.% NaCl
T_H = 218.9°C
Salinity = 3.9 eq. wt.% NaCl
T_H = 249.86°C
Salinity = 3.7 eq. wt.% NaCl
20 µm
b
T_H = 216.6°C
Salinity = 5 eq. wt.% NaCl
T_H = 206°C
Salinity = 1.7 eq. wt.% NaCl
T_H = 204.6°C
Salinity = 1.1 eq. wt.% NaCl
20 µm
c
T_H = 146.6°C
Salinity = 24.1 eq. wt.% NaCl
T_H = 145.8°C
Salinity = 24.1 eq. wt.% NaCl
T_H = 143.5°C
Salinity = 24 eq. wt.% NaCl
25 µm

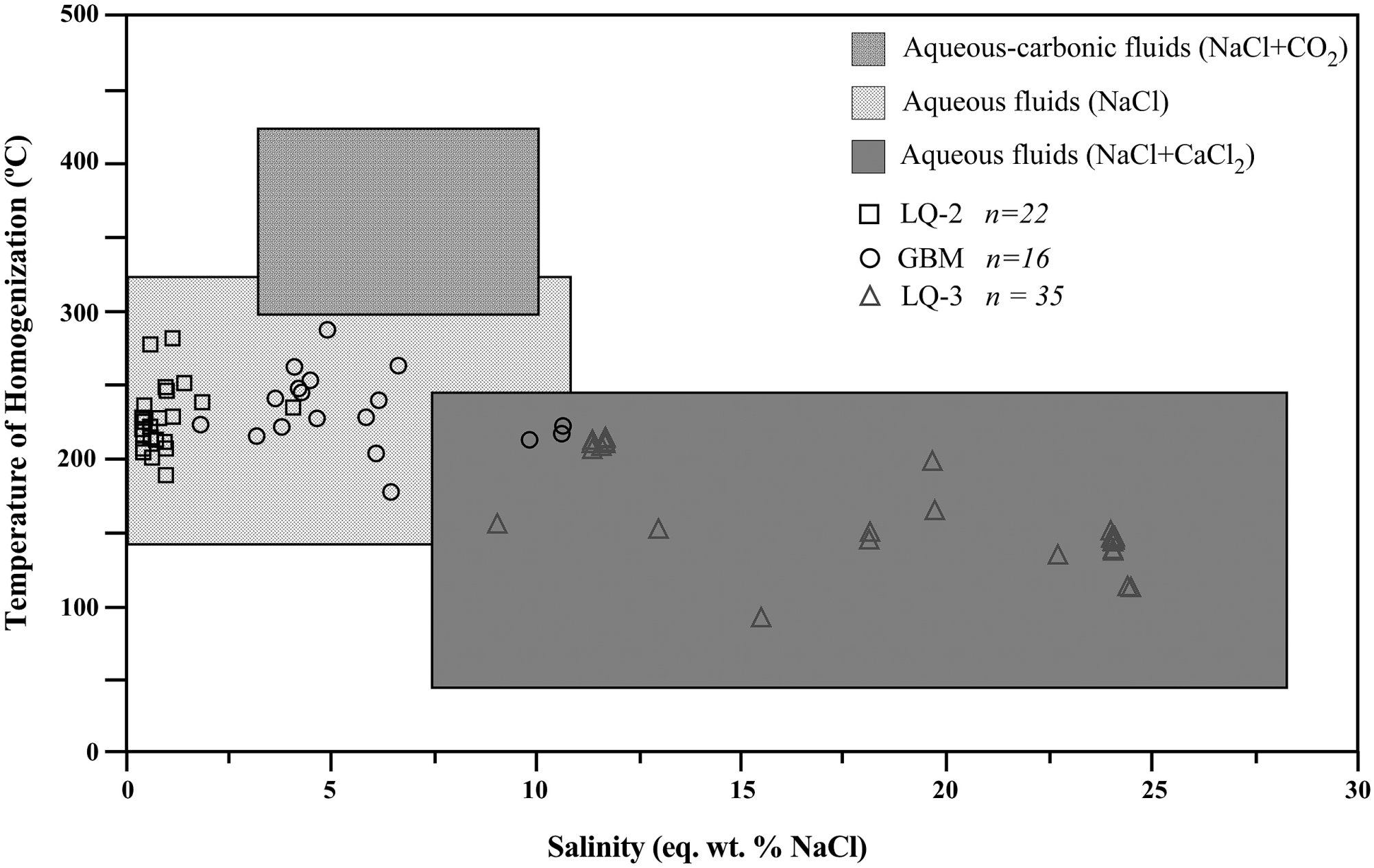
Aqueous-carbonic fluids (NaCl+CO2)
Aqueous fluids (NaCl)
Aqueous fluids (NaCl+CaCl2)
LQ-2 n=22
GBM n=16
LQ-3 n = 35
Temperature of Homogenization (°C)
Salinity (eq. wt. % NaCl)
0
100
200
300
400
500
0
5
10
15
20
25
30

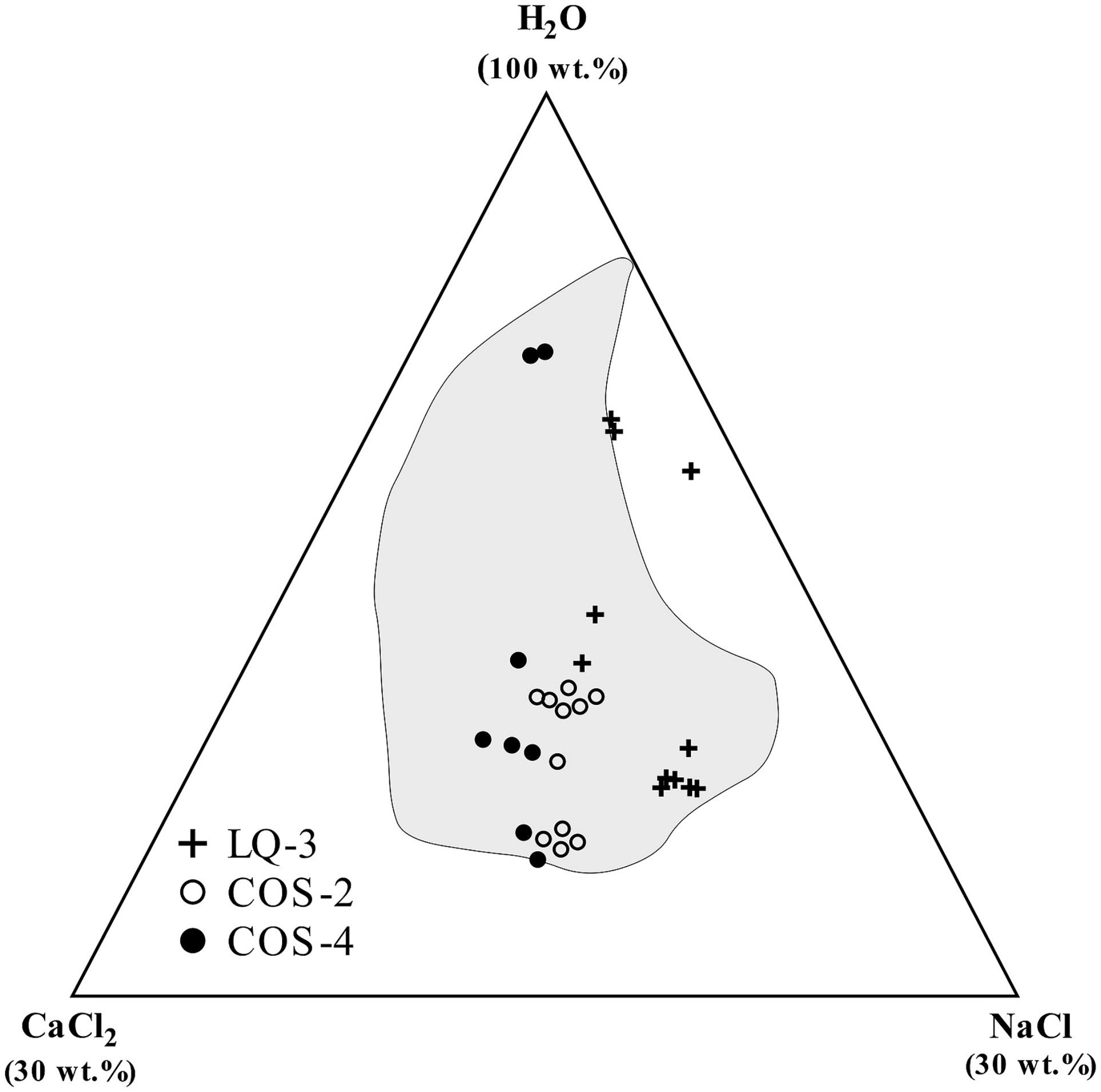
H2O
(100 wt.%)
LQ-3
COS-2
COS-4
CaCl2
(30 wt.%)
NaCl
(30 wt.%)

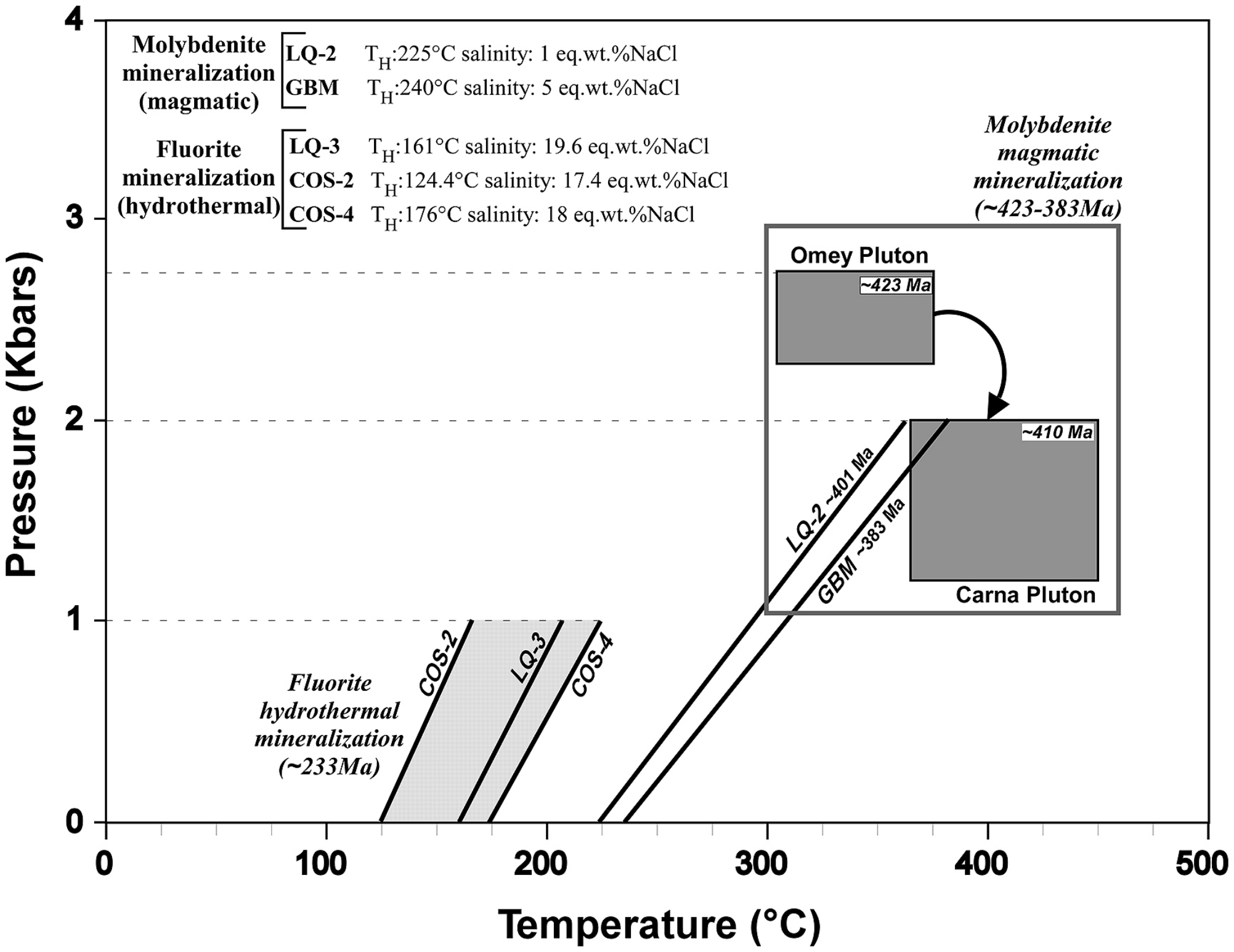
Molybdenite mineralization (magmatic)
LQ-2 T_H:225°C salinity: 1 eq.wt.%NaCl
GBM T_H:240°C salinity: 5 eq.wt.%NaCl
Fluorite mineralization (hydrothermal)
LQ-3 T_H:161°C salinity: 19.6 eq.wt.%NaCl
COS-2 T_H:124.4°C salinity: 17.4 eq.wt.%NaCl
COS-4 T_H:176°C salinity: 18 eq.wt.%NaCl
Molybdenite magmatic mineralization (~423-383Ma)
Omey Pluton
~423 Ma
~410 Ma
LQ-2 ~401 Ma
GBM ~383 Ma
Carna Pluton
Fluorite hydrothermal mineralization (~233Ma)
COS-2
LQ-3
COS-4
Pressure (Kbars)
Temperature (°C)
0
1
2
3
4
0
100
200
300
400
500

ID	Conc. U (ng)	Conc. Pb[a] (pg)	Th/U[b]	$^{206}Pb/^{204}Pb$[c]	$^{206}Pb/^{238}U$[d]	error (%)	$^{207}Pb/^{235}U$[d]	error (%)	$^{207}Pb/^{206}Pb$[d]	error (%)	ages (Ma)[d] $^{206}Pb/^{238}U$	ages (Ma)[d] error (Ma)	ages (Ma)[d] $^{207}Pb/^{235}U$	ages (Ma)[d] corr. coeff.	total common Pb (pg)
F-2	0.81	51.86	0.295	3649.94	0.065083	0.17	0.492731	0.41	0.05491	0.29	406.556	0.660	406.770	0.801	0.92
F-4	0.47	31.13	0.417	688.72	0.065203	0.20	0.495904	1.45	0.05516	1.33	407.283	0.799	408.926	0.605	2.90
F-5	0.55	37.42	0.535	609.54	0.064441	0.19	0.489411	1.66	0.05508	1.55	402.664	0.757	404.509	0.639	3.83
F-6	0.63	42.61	0.520	1349.83	0.064467	0.19	0.487842	0.80	0.05488	0.70	402.823	0.740	403.439	0.600	1.94
F-8	0.73	50.05	0.574	1768.67	0.064952	0.17	0.491973	0.64	0.05493	0.54	405.756	0.656	406.254	0.662	1.71
F-10	0.24	16.47	0.511	362.94	0.064334	0.27	0.487357	2.83	0.05494	2.65	402.019	1.067	403.108	0.669	2.91
F-13	0.32	21.25	0.444	1053.53	0.064175	0.19	0.487391	1.00	0.05508	0.90	401.058	0.726	403.131	0.570	1.27
F-17	0.26	17.45	0.472	415.61	0.064257	0.24	0.487035	2.40	0.05497	2.25	401.553	0.944	402.888	0.647	2.70
F-18	0.33	21.76	0.461	1012.58	0.064184	0.21	0.487487	1.06	0.05508	0.96	401.112	0.798	403.197	0.555	1.35

[a] radiogenic Pb.

[b] Th contents calculated from radiogenic ^{208}Pb and the $^{207}Pb/^{206}Pb$ date of the sample, assuming concordance between U-Th and Pb systems.

[c] measured ratio corrected for fractionation only. All Pb isotope ratios were measured using the Daly detector, and are corrected for mass fractionation using 0.15 %/amu.

[d] corrected for fractionation, spike, blank and Th disequilibrium. All common Pb is assumed to be blank.

All errors except error in the $^{206}Pb/^{238}U$ age are reported in percent at the 2σ confidence interval. Error in the $^{206}Pb/^{238}U$ age is reported in absolute (Ma) at the 2σ confidence interval.

TYPES	Type 1	Type 2	Type 3	Type 4
PHASES PRESENT	L+V	L	L+V+S	L+S
FILL	0.7-0.9	-	0.5-0.9	-
SHAPE	rounded to negative crystal shape	rounded to negative crystal shape	rounded to negative crystal shape	rounded to negative crystal shape
SIZE (μm)	<2 to 200	<2 to 100	5 to 200	5 to 100
DISTRIBUTION	Clusters and isolated	clusters and trails	clusters and isolated	clusters and trails
GRANITE QUARTZ	XXX	XX	X	-
MOLYBDENITE VEIN QUARTZ	XXX	XX	-	-
VEIN FLUORITE	XXX	XX	XX	XXX

Sample	T_{FM} (°C)	T_{Mhyd} (°C)	T_{LM} (°C)	T_H (°C)	Eq. wt.% NaCl	Eq. wt.% $CaCl_2$
Molybdenite Vein Quartz (GMB)	-26.5 to -19.8 (Av. -23.4) *n=5*	-	-7.1 to -1.1 (Av. -3.3) *n=16*	176 to 284.3 (Av. 232) *n=16*	1.9 to 10.6 (Av. 5.3) *n=16*	-
Molybdenite Vein Quartz (LQ-2)	-28 to -20 (Av. -26) *n=12*	-	-3 to -0.2 (Av. -0.5) *n=22*	187.6 to 281.5 (Av. 223.8) *n=22*	0.4 to 5 (Av. 0.8) *n=22*	
Vein Fluorite (LQ-3)	-57 to -48.2 (Av. -54.3) *n=35*	-25.3 to -22.1 (Av. -23.8) *n=32*	-23.5 to -5.9 (Av. -17.0) *n=35*	90.6 to 214.0 (Av. 160.8) *n=35*	9.1 to 24.6 (Av. 19.6) n=35	1.6 to 8.8 (Av. 6.2) *n=32*

Sample	wt(g)	Re (ppm)	±	187Re (ppm)	±	187Os (ppb)	±	Age	±^	±*	±#
RO1047-1_LQ-5-2	0.030	161.28	0.55	101.37	0.35	679.52	1.91	401.0	0.2	1.6	2.0

^uncertainty including only mass spectrometry uncertainty
*uncertainty including all sources of analytical uncertainty
#uncertainty including all sources of analytical uncertainty plus decay constant

A review of molybdenite, and fluorite mineralization in Caledonian granite basement, western Ireland, incorporating new field and fluid inclusion studies, and Re-Os and U-Pb geochronology.

Martin Feely[1]*, Alessandra Costanzo[1], Sean P. Gaynor[2,3], David Selby[4] and Emma McNulty[1]

[1] Geofluids Research Group, Earth and Ocean Sciences, School of Natural Sciences, National University of Ireland Galway, Galway, Ireland
[2]Department, of Geological Sciences, University of North Carolina at Chapel Hill, Chapel Hill, North Carolina, 27510, USA
[3]*Now at* Department of Earth Sciences, University of Geneva, rue des Maraîchers 13, Geneva, Switzerland
[4] Department of Earth Sciences, Durham University, Durham, UK

Highlights

- New discovery of late-Triassic gem quality fluorite in Connemara, Ireland.
- Late-magmatic quartz vein-hosted molybdenite in the Caledonian Galway Granite.
- 40My period of molybdenite mineralization.
- New geochronometry (Re-Os, U-Pb) and fluid inclusion studies from the GGC.